to Astronomical Journal

Metallicity Gradients in Elliptical Galaxies

Patricia C. Hanlan
Department of Astronomy, University of Michigan

James M. Schombert[1]
Infrared Processing and Analysis Center, Jet Propulsion Laboratory
California Institute of technology

Mary Barsony[1]
Harvard-Smithsonian Center for Astrophysics

and

Karl D. Rakes
Institute for Astronomy, University of Vienna

ADSTRACT

Narrow band optical and near-IR images are used to study color gradients in elliptical galaxies. Over 90% of the 23 galaxies observed display gradients at the level equivalent to $\Delta Mg_2/\Delta \log r = -0.043 \pm 0.017$ or $\Delta Mg_2/\Delta \mu_V = -0.015 \pm 0.007$. Near-IR colors imply $\Delta[Fe/H]/\Delta \log r = -0.44$ and core [Fe/H] values between 0.0 and 0.3 versus halo values near *–0.8. The* discrepancy between optical colors, influenced by light element abundances (particularly CN), and $J - K$, which is dominated by the true metallicity as reflected in the mean GB temperature, suggests the hypothesis proposed by Worthey, Faber and Gonzalez (1 992) is correct, that the [Mg/Fe] ratio in ellipticals differs from other galaxies due to an enhanced Type 11 SN component at the initial phase of star formation. Whereas, most galaxies display gradients, some galaxies display a two component gradient structure with strong core gradients and weak halo gradients, similarly to those first noticed by Thomsen and Baum. This implies that, spatially, the early star formation histories in ellipticals are more complicated than the standard scenarios of galaxy formation predict, such that there existed an early phase of star formation which was slower than the timescales for gas infall. This produced an inner region with a strong [Fe/H] gradient whereas weak halo gradients originated from either a later phase of slower star formation or mergers with less massive neighbors. Gradients in our continuum color, $b - y$, signals a BHB population contribution in the integrated light and warns that finer knowledge of the color evolutionary history of ellipticals will require substantial improvements in our SED models in order to predict behavior from the far-UV to the near-IR.

Subject headings: galaxies: photometry - galaxies: evolution - galaxies: formation - mass-luminosity relation

[1] Visiting Astronomer, Kitt Peak National Observatory. KPNO is operated by AURA, Inc. under cooperative agreement with the National Science Foundation

I. Introduction

The relationship between color and luminosity for galaxies, as well as color gradients within galaxies, reflects the complicated interplay between star formation history and chemical evolution in systems with composite stellar populations. However, in single generation objects, such as elliptical galaxies, a unique age to the stellar population implies that color variations arc primarily metallicity dependent. Although we have increasing evidence that elliptical are more than a simple, single generation stellar population (Rose 1985, Worthey 1992), theoretical work on the spread of chemical abundance in stars produced during the initial star burst (Arirnoto and Yoshii 1986) demonstrates that metallicity gradients arc still a powerful probe into the details of galaxy formation regardless of age complications.

The study of metalicit y gradients is an examination of the relics of the first epoch of star formation and, thus, another issue that metal licity gradients can address is the relationship between chemical and dynamical evolution during the initial phase of star formation. Formation gas is enriched by the ejecta from first generation stars. This gas cools and dissipates causing metal enriched gas to become more centrally concentrated, Subsequent star formation freezes the distribution of mean [Fe/H] into the angular momentum of the stellar orbits with lower metallicity stars on higher angular momentum orbits (Larson 1975, Gott and Thuan 1976, White 1980, van Albada 1982). As the late stages of stellar evolution dominates the integrated luminosity of the galaxy, these metallicity differences are reflected into color gradients. '1'bus, the strength of color gradients is directly related to the rate and style of star formation during galaxy formation. The standard galaxy formation models predict high [Fe/H] values and high metallicity gradients (Thomsen and Baum 1989), whereas dynamical evolution, such as mergers, serves to lower gradients (Peletier, Valentijn and Jameson 1990).

In order to examine the chemical evolution in ellipticals, one would like to obtain line information on various spectral features as a function of radius. But, since line gradient work was impossible in the early years, initial work concentrated on the usc of aperture photometry (dc Vaucouleurs and dc Vaucouleurs 1972, Sandage and Visvanathan 1978, Frogel *et al.* 1978) and photographic material (Strom *et a/. 1976)* using filters sensitive to regions dominated by metal lines (e.g. the near-blue). These studies demons. trated that most early type galaxies have blue gradients as predicted by early models of galaxy formation. With the advent of linear areal detectors (i.e. CCD's) numerous studies acquired highly accurate data, usually in a broadband Johnson system (Franx and Illingworth 1990, Peletier *et al.* 1990, Jedrzejewski 1987, Boroson and Thompson 1987, Cohen 1986, Davis *et al.* 1985) and with the recent development of near-hi arrays, more work has extended the observational database with near-IR JHK photometry (Peletier, Valentijn and J ameson 1990, Silva and Elston 1983). All these studies can be summarized in that they confirm the early aperture work on blue gradients with two important enhancements: 1) the gradients found are modest, only on the order of $A(U - B)/\Delta \log r$ = –0.1 1 corresponding to Δ[Fe/H]/$\Delta \log r$ = –0.3 and 2) some galaxies exhibit a two component gradient (strong core, weak halo).

The above color work was confirmed by line strength work (Faber, Burstein and Dressler 1977, Gorgas, Efstathiou and Salamanca 1990, Davidage 1993) but fcw of these studies were able to reach deep into elliptical halos. On the other hand, broad band colors can be severely hampered by non-metallicity effects within the stellar population. For example, a small metal-poor population with a mean [Ire/ll] < — 1.5 can severely hamper broadband analysis from $B - V$ colors due to a strong blue horizontal branch (BHB) contribution. The degeneracy between age and metallicity is well known (see Burstein 1985 for a review) and cannot be resolved in broad band systems. The usual solution is either the usc of spectral indices (Gorgas, Efstathiou and Salamanca 1990, Thomsen and Baum 1989) or long baseline colors to distinguish between main sequence and giant branch stars (i.e. V - K, Persson, Frogel and Aaronson 1979). This study attempts a slightly modified approach combining a narrow band blue photometry system with near-l}t imaging, thus maintaining the two dimensional information at the sacrifice of spectral resolution with the eventual aim of directly comparing the metalicity results from cool giants (near-llt) with non-degenerate narrow band indices in the line blanketed near-blue region of the spectrum. Our goal, then, is twofold: 1) compare the differences in the contribution of the underlying stellar population in ellipticals from the optical to the near-Ilt as a test of galaxy formation and evolution theory and 2) link the colors to spectral indices in order to determine the chemical evolutionary history of ellipticals both globally and spatially.

Cosmological parameters of H_o = 100 km See^{-1} Mpc^{-1}, Ω_o = 0.2 and a Virgo distance of 14.5 Mpc are adopted for this study.

11. Observations

a). Optical

The optical data for this study were obtained on Michigan-Dartmouth-MIT's 1.3m telescope located on the southwest ridge at KPN O. The CCD device used was a Thomson CSF with a plate scale of 0.48 arcsec pcr pixel. This device has 30% QE at 3500Å, 80% QE at 5500Å and excellent flattening characteristics. Rest frame Strömgren *uvby* images were obtained using a filter set devised for the study color evolution of distant clusters (see Rakes, Schombert and Kreidl 1991) and are easil y obtained from commercial optical manufacturers. Exposure times ranged from 600 to 900 sccs and calibration used standards from Perry, Olsen and Crawford (1 987). Although the Strömgren system is a color system, the standards from Perry, Olsen and Crawford contain a Johnson *V* value allowing the conversion of the y data to a standard flux zeropoint.

The Strömgren narrow band system was chosen to avoid some of the ambiguity generated by broad band filter systems such as Johnson *UBV*. The intent is to apply the resulting color indices to a homogeneous group of objects (bright ellipticals) to search for subtle differences. in this context, the optical filters are selected to be sensitive to various regions of interest relative to an object composed primarily of an old, metal-rich stellar population. The *u* filter samples the near-UV portion of the spectrum at 3500Å. The v filter is centered on the Fe-CN blend at 4100Å. The *b* and y filters arc selected to avoid any features and serve as continuum benchmarks. These filters are shown in Figure 1 along with a spectrum of a bright elliptical.

The data were reduced to 1 D surface photometry in all bandpasses using the software package ARCHANGEL (Schombert *et al.* 1989). Colors were determined by three methods: 1) luminosity weighted integrated color, a mean color weighted by the y isophote, 2) metric colors, colors within an aperture in kpc and 3) multi-color surface photometry, color as a function of radius for gradient analysis. The luminosity weighted colors listed in Table 1 are used as the galaxy color unless noted in the text. In general, the errors in the colors were calculated based on reduction of separate frames. These analysis produced mean errors on the luminosity weighted colors to be ± 0.06 in $u - v$, ± 0.04 in $v - y$ and ± 0.03 in $b - y$. Error bars on the surface photometry are based on RMS values around the ellipse in question as well as a component duc to the uncertainty of the sky value. Mean colors and dispersions for the sample are given in Table 2. Blue magnitudes, velocities and extinction values were taken from NED (N ASA/Extragalactic Database, Helou *et al.* 1991) and all the data were corrected for Galactic extinction and redshift effects using the prescriptions of Schneider, Gunn and Hoessel (1983). Gradients were calculated try making a linear fit to a subjective region between the limits set by seeing and were sky errors dominated the outer colors. Fits were made to upper and lower errors to determine tile error on the gradients.

b). Near-lR

The near-]lt data for this study were obtained on the KPNO 1.3111 using two devices; IRIM, an SBRC 62x58 InSb array plus reimaging optics for a plate scale of 1.35 arcsec per pixel and SQIID, a four component camera using separate Hughes 256x256 hybrid platinum silicide arrays. Both cameras were calibrated using Elias *et al.* (1982) standards and were corrected for non-linearity using prescriptions found in the NOAO manuals. The IRIM data was taken in a series of ten 60 scc exposures through J (1 .25μm), H (1 .65μm) and K (2.2μm). Due to the limited sky coverage for this array, a cross pattern mosaic was used to check that the real sky level was achieved. The data was flattened using mean sky frames taken between object frames. The SQIID data was taken in series of 180 scc exposures ofl'set to sky every fifth exposure for sky flats. The lower QE on SQIID required much longer total exposure times to achieve the same surface brightness depth as IRIM, however, the larger field of view and simultaneous color information reduced the actual overhead so that a comparable number of objects was obtained with SQIID as IRIM. The near-IR data arc less deep in surface brightness than the optical data since ellipticals are typically 4 times more luminous at K than at V (5500 Å), but the sky is 10,000 times brighter. Typically the K data was good to 0.1% of sky which corresponds to 19 K mag arcsec^{-2} or 22 V mag arcsec^{-2}. Error analysis was similar to the optical colors, based on multiple exposures reduced separately. The mean errors in V — K and $J - K$ were ± 0.06 and ± 0.04. These near-l]t passbands arc the standard JHK system and their characteristics, with respect to elliptical, are reviewed in the series of papers by Persson, Frogel and Aaronson (1 979) (see Figure 1). This region of the spectrum is particularly sensitive to cool, luminous giants and serves to indicate age, metallicity and recent star formation when compared to optical colors (see Bothun 1990). in total, nine ellipticals were imaged with SQIID and six with IRIM. The data was reduced to 1 D surface photometry exactly the same way as the optical data. All the data were corrected for Galactic extinction and redshift effects using the prescriptions of Thuan and Puschell (1989).

c). Mg_2 system and [Fe/H] in ellipticals

The idealized situation in the study of abundances, and global chemical evolution in galaxies, is knowledge of the value of Z, the mass fraction of elements heavier than helium, as a function of position and time. Rowever, this is clearly impractical and one usually resorts to quantifying [Fe/Ii] to a spectral index using solar system standards. In this regard, one of the more common indices in use for elliptical is the Mg triplet feature at 5200Å. The usual expression of the Mg triplet is the Mg_2 system (Faber *et al.* 1989) which has been used in several gradient studies (Gorgas, Efstathiou and Salamanca 1990, Thomsen and Baum 1989). In addition, recent work by Buzzoni, Gariboldi and Mantegazza (1992) and Worthey (1992) provide a new calibration from Mg_2 to [Fe/H] as well as to $V - K$ and J – K in elliptical.

The first step in comparing our photometry system to [Fe/1 1] is a comparison of Mg_2 to our metallicit y indicator, v — y. This relationship is shown in Figure 2 where the Mg_2 values of 15 galaxies are taken from Faber *et al.* 1989 and $v - y_o$ colors are produced from the region within the galaxy which matches the size of the slits used to determine Mg_2. Ellipticals are separated into cooling flow objects and normal elliptical; however, no difference was detected between these types (see below). A linear fit to this relations gives

$$Mg_2 = 0.24(v - y) \text{ --}0.09. \quad (1)$$

And using the relation of Mg_2 to [Ire/II] from Buzzoni, Gariboldi and Mautegazza (1992) gives

$$[Fe/H] = 1.776(v - y) - 2{,}741. \quad (2)$$

On the other hand, using the calibration from Worthey (1 992), who adopts a larger dependence between Mg and Fe for red giants gives

$$[Fe/H] = 1.118(v - y) - 1.856. \quad (3)$$

Worthey 's calibration is somewhat more confident since actually Fe lines and model atmospheres are used. This comparison of metallicity values assumes that the ratio of Mg to Fe is unity. Recent evidence, presented by Worthcy, Faber and Gonzalez (1992) suggests that [Mg/Fe] exceeds this value by 0.2 dex signaling an enhanced contribution from Type II SN's. This problem with Mg abundant.c can be avoided by directly calibrating $v - y$ color, which measures the CN band, to [Fe/11], however, there arc too fcw galaxies with direct spectroscopic determination of Fe to perform this task. We do note that the slope of $v - y$ to Mg_2 is exactly the same as $V - K$ to Mg_2 from Buzzoni, Gariboldi and Mantegazza (1992). This situation is even more complicated if one considers the globular cluster calibrations presented by Brodie and Huchra (1990), where their conversion from Mg_2 to Fe gives

$$[Fe/H] = 2.38(v - y) - 3.10. \quad (4)$$

However, this calibration is only presented up to a [Fe/Ii] value of –0.5 and was never intended to calibration solar, or greater, metal] licities. Worthey's models produce an excellent fit to tile globular cluster data and indicate a sharp rise in Mg_2 to Fe slopes beyond [Fe/H]=–0.5. This is a similar problem for our near-I1t calibration of metallicity, $J - K$, where Worthey calculates for greater than [Fe/H]= –0.5

$$[Fe/H] = 3.17(J - K) - 3.16 \quad (5)$$

whereas, Brodie and Huchra calculate

$$[Fe/H] = 5.57(J - K) - 5.20 \quad (6)$$

for globular clusters. Again, the Worthcy models match the low metallicity end of the sequence and then predict a sharp rise at [Fe/H]=–0.5. For our discussion wc will adopt the Worthey calibration and in §III wc will determine an empirical calibrations from Mg to Fe using the above v – y calibration and model calibrated $J - K$ colors. At the very least, wc can confirm the relation between onc light element color, v – y and the CN blend, and another light element, Mg.

'J'here is little spatial Mg_2 data in the literature, primarily from Grogas, Efstathiou and Salamanca (1990). However, a recent study by Davidage (1992) produced Mg_2 data in NGC 2693 out to 15 arcsecs which can be directly compared to the colors in this study. Figure 3 shows the comparison between Davidage and this study for v – y colors in NGC 2693 converted to Mg_2 using the above relation. The agreement between the narrow band colors and Davidage's spectral features is good, and again reinforces our belief that we can reproduce Mg_2 values with v — y colors.

III. Results

The photometric results of this study are summarized in "1'able 1. Mean colors were determined by a luminosity weighting algorithm based on the V surface brightness of each contour. Core v – y colors $(v - y_o)$ represent integrated colors within 2 arcsecs for comparison to core Mg_2 values in §IIc. Near-l R integrated colors arc also listed in Table 1 weighted by J surface brightness. Also listed are absolute blue magnitudes based on velocities extracted from NED and the color gradients expressed as change in magnitude per log radius (see Lc1ow). The histograms of these colors are found in Figure 4 with tile mean values for the optical colors found in 'J'able 2. Mean near-IR colors do not differ significantly from the values obtained in the pioneering studies by Persson, Frogel and Aaronson (1979). Note that the only SO in the sample, NGC 7332, has markedly bluer colors due to a contribution from a younger disk population (see Bothun and Gregg 1990). Once corrected for the color-magnitude (CM) effect (see below), the dispersion is solely duc to observational error and the effects of strong color gradients. An exception to this homogenity is that the galaxies which exhibit strong X-ray emission or actual cooling flow phenomenon have slightly redder, but statistically significant, $V - K$ colors. This will be discussed further in a separate paper (Schombert, Barsony and Hanlan 1993) and the cooling flow galaxies arc marked as a reference for the reader, but were not excluded from the analysis, The mean colors in Table 2 will also be used in a later paper to define the zero epoch characteristics of ellipticals in a study of color evolution from z=O to z= 1 (Rakes and Schombert 1993).

The color-magnitude relations are shown in Figure 5 using luminosity weighted integrated colors and total blue magnitudes. The u – y and v – y colors display clear correlations with absolute luminosity in a similar manner and magnitude as the old $U - V$ and B – V correlations (Visvanathan and Sandage 1977, Griersmith 1982). The near-l]t colors also display the expcctcd correlations, although $J - K$ exhibits a more significant relation than V — K. This is due, somewhat, to the peculiar red $V - K$ colors displayed by cooling flow galaxies, but the normal ellipticals also display a weaker correlation of luminosity with V – K versus J – K. Note that $b - y$ displays no correlation with luminosity. The various linear fits for each color are also found in Figure 5, as well as the errors on the fits.

Significant gradients were found in 22 out of 23 elliptical (95'%) in the optical and 13 out of 15 (88%) in the near-IR surface photometry. The color profiles arc shown in Figures 6, 7 and 8 for the colors v – y, J – K and the cross band color $V - K$. Gradients, expressed in units of Δcolor/$\Delta \log r$, and their errors arc listed in Table 3 and arc based on linear fits to intermediate regions of the color profiles to minimize distortions due to seeing errors in the core and large error bars in the halos. In genera], the same features are seen in the color profiles for all color indices (exceptions are NGC 507 and NGC 6702 which display sharper gradients in $J - K$ than v – y). The gradients in $V - K$ and v – y arc weakly correlated; however, none of the gradients are strictly linear in log r space and many galaxies exhibit a two component nature in their color profiles which prohibits a direct comparison of the gradients in different filters (see below). Mean gradients arc $\Delta(v - y)/\Delta \log r$ = –0.18 ± ().08 and $\Delta(b - y)/\Delta \log r$ = —0.09 ± 0,04. In terms of a dimensionless surface brightness index (Thomsen and Baum 1989), the mean gradient for ellipticals was $\Delta(v - y)/\Delta\mu_V$ = –0.06 ± 0.03. Relating the v – y index to the Mg_2 system from §IIc produces mean gradients for the normal elliptical sample of $\Delta Mg_2/\Delta\mu_V$ = –0.015 ± 0.007, which is slightly shallower than the gradients found in three Coma ellipticals in a study by Thomsen and Baum (-0.032, -0.023 and -0.020).

The gradients in $J - K$ and V–A' are also listed in Table 3 with mean values of --0.13±0.09 and –0.30±0.19 respectively. These values confirm the work by previous studies in that color gradients are relatively weak in ellipticals (Cohen 1986, Boroson and Thompson 1987, Franx and Illingworth 1990). Gradients from older studies were typically –O. 10 in $B - R$ which corresponds to –0.18 in $v - y$, in good agreement with the mean gradient in this study. The conversion of V – K to [Fe/11] from Buzzoni, Gariboldi and Mantegazza (1992) implies the same slopes as v – y. However, the mean $J - K$ gradient implies a Δ[Fe/H] that is a factor of two higher

than calculated from the v – y or $V-K$ colors. Using the calibration from Worthey (1 992) produces a similar discrepancy between v – y and $J-K$, so we conclude the difference is real and not model dependent,

There is a correlation between color gradient and v – y color in the sense that red galaxies have steeper gradients (see Figure 10). But, there is no corresponding correlation for $b-y$ and only a very weak correlation in $J-K$ (but in the opposite sense, red galaxies have shallower gradients). The v – y correlation is even stronger if core v – y values are used instead of integrated colors. Due to the CM relation, this correlation, by default, implies that brighter, or more massive, galaxies have steeper gradients for colors that measure light elements rather than total metallicity.

Several galaxies display more complicated structure in their color profiles that can be fit by a simple linear relation. In fact, these galaxies (see NGC 6703 and NGC 7626 in Figure 9) universally have steeper inner profiles and weak halo gradients. This was also seen in Thomsen and Baum (1 989) for their Mg_2 profile of NGC 4839. This is often more obvious when color is plotted against surface brightness, μ_V, as proposed by Thomsen and Baum, since values compared in log r space tend to blur the core colors compared to halo values. All the galaxies with double components have similar patterns in that they all have steep core gradients connecting to shallow halo gradients. The separation into inner and outer gradients is quite sharp and indicates a distinct mechanism that decoupled the outer and inner stellar populations.

in the 2D data, the position angles and eccentric.ity of the Lest-fit ellipses matched, to within the errors, for each bandpass from 3500Å to 2.2μm. In other words, the isophotes match the isochrones in every color. However, this result is restricted to the high S/N regions, typically 1/2 to onc r_e since the algorithms that determine best fit ellipse become unstable at 5% of the sky value. There is a theoretical expectation that isochromes be more flattened than isophotes (Larson 1975, Carlberg 1984), which is not seen in this data set.

IV. Discussion

The unique advantage of the Strömgren colors to the study of color evolution in galaxies is outlined in Rakes, Schombert and Kreidl (1991). Briefly, the $u-y$ color is a measure of recent star formation as signaled by blue colors from massive O and B stars, v – y is a metallicity indicator based on the CN blend at 4170Å (see Dell, Hesser and Cannon 1983) and $b-y$ *is* a continuum measure, which for elliptical is a mean color of the composite turnoff main sequence stars and sub-giants (Rose 1985). In addition, the u – v color serves as a measure of the 4000Å break, an age indicator and a standard probe in color evolution of distant galaxies (Spinrad 1986, Hamilton 1985). The meaning of the near-IR colors are described in Persson, Frogel and Aaronson (1979) with respect to ellipticals and are primarily a measure of the dwarf to giant ratio $(V-A')$ and the mean metal licity of the giant branch $(J-A')$. However, the mean age of the stellar population, particularly a contribution by AGB stars is also relevant. The above interpretation is, of course, simplistic and naive and makes many assumptions about the 1 MF, star formation history and the amount of recent star formation and thus, when relevant to the discussion, we have been guided in our interpretation of our narrow band and near-IR colors by a series of spectroenergy distribution (SED) models available in the literature (Bruzual 1983, Arimoto and Yoshii 1986, Guiderdoni and Rocca-Volmerange 1987, Worthey 1992) and by results for the optical filters from high redshift samples (Rakes and Schombert 1993).

A traditional understanding of the global metallicity in ellipticals has come from the color-magnitude (CM) relation (Visvanathan and Sandage 1977, Griersmith 1982). This relation reflects the mass- metallicity correlation expected if ellipticals are a single burst population where the total product of metals is proportional to the number of supernovae initially present, thereby relating the number of stars to the total mass of the galaxy. In turn, the number of SN determines the amount of gas heating for the onset of galactic winds which are balanced by the gravitational potential of the galaxy. q'bus, the mean metallicity of the underlying stellar population is reflected into the integrated color by the increased opacity of giant stars, which lowers the mean temperature, and line blanketing, which decreases the flux in the near-b]uc, such that massive, metal-rich ellipticals are redder than their smaller, metal-poor cousins. These relations, for all the colors used herein, are shown in Figure 5. For comparison, tile slope of the mass-metallicity relation in B – V is –0.038 and in $U-V$ it is —0.126 (Griersmith 1982). Assuming a constant M/L for elliptical (Faber and Gallagher 1979, Michaud 1980) and that Mg_2 traces the total metal content of a galaxy, Z, then the slope for the v — y colors gives $Mass \propto Z^{5.2\pm1.9}$ using the calibrations from Buzzoni, Gariboldi and Mantegazza (1992) or $Mass \propto Z^{7.7\pm2.1}$ using the calibration from Worthey (1 992). This represents a change in [Fe/H] from O, the solar value, at M_B = --18 to +0.3 for the

highest luminosity galaxies. On the other hand, the mass-metallicity relation calculated from J -1< colors produces $Mass \propto Z^{4.6\pm0.9}$.

The differences between estimates of total metallicity, Z, from v – y and $J-K$ may reflect the different methods of sampling the mean metallicity of the underlying stellar population. This has recently been noted by Silva and Elston (1992) in a parallel near-IR study. For example, $J-K$ samples the mean temperature of the giant branch as governed by the opacity of the stars driven by the number of free electrons, a quantity directly proportional to Z. On the other hand, v – y measures primarily the CN blend a light clement measure of metallicity strength. In §IIc, wc have related v – y color to Mg_2 with high agreement. However, Mg_2 and other light elements may not be direct indicators of [Fe/n] and, thus, Z. In recent work, by Worthey, Faber and Gonzalez (1 992), model indices were compared to detailed elliptical spectra and they conclude that the [Mg/Fe] ratio differs in elliptical in a manner such that the lighter elements are more abundant due to differing enrichments from Type 11 SN's during the epoch of first star formation. Thus, our data would support the observations of Silva and Elston (1 992), and the Worthey, Faber and Gonzalez models, since our v – y colors indicate a increasing dependence on mass which is much stronger than the same relation determined from $J-K$ colors and which could be caused by an overestimate of [Fe/11] from light elements, such as C and N, versus true Z dependence based on giant branch temperatures. This same behavior is also seen in the color gradients (see below).

If wc adopt Worthey 's most recent calibration of $J-K$ to [Fe/H] as a measure of Z, and take the v - y values converted to Mg_2, then an empirical calibration from Mg_2 to [Fe/H] yields a slope of $dMg_2/d[Fe/H] = 0.11$. This is lower than the model slopes in the literature which range from 0.14 for Buzzoni, Gariboldi and Mantegazza (1992) to 0.26 from Worthey (1 992). This also implies that tile light to heavy clement abundances (i.e. Mg/Fe) must change by a factor of two over the range of galaxy masses studied herein such that light elements are overenhanced in giant elliptical. '1'bus, we adopt the value of $Mass \propto Z^{4.6\pm0.9}$ from our J — K colors to represent the true change in total metallicity.

The $b-y$ colors display no correlation with luminosity and the b – y index should be less sensitive to metallicity than any broad band near-blue colors, such as $B-V$, because the b ancl y filters arc chosen to avoid any metal features, although this is not strictly true since any region of the near-blue spectrum has numerous weak metal lines. In addition, this portion of the spectroenergy curve in ellipticals is more sensitive to sub-giants and turnoff stars than giant branch stars (Rose 1985) and, therefore, is also less sensitive to metallicity effects that change a star's position in the HR diagram. All of this implies that $b-y$ is only mildly sensitive to mean metallicities, and more dominated by the composition of the subgiants (i.e. the dwarf to giant ratio). '1'bus, the lack of correlation with luminosity is not surprising, but also states that the mean age of ellipticals, is highly similar since the low dispersion in b – y must reflect a low dispersion in the color (age) of turnoff stars and a similar mean IMF between ellipticals. This agrees with the analysis by Wyse (1985), that ellipticals arc formed by a short burst of star formation at a similar epoch.

The u – y colors also show a low dispersion and no star formation involving massive stars is indicated as onc would expect from the obvious old, gas-free nature of ellipticals. However, the colors arc too blue for any expectation based on SED models in the literature. This is also not unexpected since ellipticals have long been unexplained in the UV (see Burstein *et al.* 1988), but this is usually only detectable in the far-UV. It has previously been unclear whether this is a metallicity effect, (although this would indicate a low, not high, metal population dominating the UV) or some contribution from a blue 1111 population or exotic population such as PN core stars. Our arguments below leads us to believe that a weak BHB contribution, which is minimal at 5500Å, yet substantial in the hotter UV, is the underlying contributor to the $u-y$ colors.

The behavior of the colors and their small dispersion agrees with previous studies in interpreting ellipticals as an old population with little star formation or reddening effects. This behavior is also confirmed in work using the Strömgren filters to trace color evolution with redshift (Rakos and Schombert 1993). That study also found a relationship between continuum colors that closely match the expected theoretical values for a simple, single generation stellar population as it evolved with time as predicted from the SE]) models of Guiderdoni and Rocca-Volmerange (1987). In addition, it was found that the b – y colors follow the single age population models closer than $v-y$ which signaled a metallicity effect and the changing contribution from metal poor stars at various epochs to the $v-y$ colors. '1'bus, wc will continue to interpretate the changes in colors with radius as a metallicity effect rather than a age or recent star formation problem.

As anticipated from the known characteristics of ellipticals, the core properties seen herein are indicative of an old, metal-rich stellar population. The core v – y values are listed in 'l'able 1. The mean value is 1.59 ± 0.08 which represents a [Fe/H] of +0.03 based on calibration from Worthey (1992). The distribution of core [Fe/H], based on v – y values, are shown in Figure 11. Halo metallicities based on colors measured at r_e, the half-light radius, are also shown in Figure 11. Extrapolating colors from r_e to the Holmberg radius (26 B mag arcsec^{-2}) gives a typical outer halo metallicity of –0.8. The mean value of –0.8 lies above a value for the metallicity of a halo Pop 11 system of our Galaxy and serves as an important constraint in galaxy formation theory since the lowest [Fe/H] represents the metallicity of the earliest generation of stars and defines the timescale of early star formation. Globular cluster systems in elliptical have lower [Fe/H] than halo stars at same radius (Mould, Oke and Nemec 1987), unlike the stars in our own Galaxy halo which have a typical [Fe/II] = – 1.5 (Carney 1988). This would strengthen arguments that globulars around elliptical have their origin as captured systems from past merger events. The core [Fe/11] value also appears to have an upper limit at +-0.4. This maximum metallicity is a prediction from several numerical and analytical solutions where the maximum value of Z matches the yield from stars (Tinsley 1980, Arimoto and Yoshii 1986).

Color gradients reflect the details of the formation processes where infalling gas is enriched by mass loss from stars. Dissipation causes the higher metallicity gas to flow inward where later star formation freezes the mean [Fe/H] value (and thereby color) into the stellar orbits resulting in these gradients (Larson 1975). The gradients in v – y and $J-K$ are expected to be the strongest since they actually measures a metallicity feature or phenomenon and this is true in the data. "l'he $v-y$ gradients correspond to $\Delta Mg_2/\Delta \log r$ = –0.044 ± 0.024 which translates into Δ[Fe/H]/$\Delta \log r$ = —0.22 ± 0.07 using tile Worthey (1992) calibration. The gradients implied from the J — K colors are Δ[Fe/H]/$\Delta \log r$ = —0.44 ± 0.25, a factor of two greater. This is similar to the discrepancy found from the CM relation between v – y and $J-K$ and, again, wc feel this signals a decoupling of lighter versus heavy element abundance estimates, such that the heavy clement gradients are steeper. As stated in $111, the gradients measured, when converted to [Fe/11] are, in genera], modest. However, recent models have been developed which predict these behavior based on chemodynamical N-body simulations that includes a primordial mixture of warm and cold dark matter (Stiavelli and Matteucci 1991), For a galaxy of $10^{11} M_{\odot}$ these models predict gradients of Δ[Fe/H]/$\Delta \log r$ = –0.11, which is about 1/4 the values found by this study, and $\Delta Mg_2/\Delta \log r$ = –0.05 which is very close to the gradients measured in v – y.

The $b-y$ colors also show radial gradients, although at a lesser degree then v – y or the near-IR colors. This is somewhat surprising since there is no CM relation for $b-y$ and b – y does not correlate with Mg_2 (as would be expected since the filters were chosen to avoid spectra] features). There will always be at least a weak dependence on metallicity since lower Z will push turnoff stars and sub-giants blueward in mean temperature (although not as dramatic as changes in giant stars). To quantify this effect, a comparison with SED models and the standard stars was performed and $b-y$ was found to be a factor of ten less sensitive to metallicity than v -y. However, the typical b – y gradient observed herein is as large as 1/2 the v – y value. If we rule out metallicity, then the remaining possible factors are age gradients or peculiarities in the stellar population. Age is an unlikely possibility since the mean dispersion on the sample of in b – y is very small, indicated a similar age over a range of masses, and there is no correlation between luminosity and gradient slope. A more likely candidate for the blue gradients in b – y are changes in the stellar content from a core, metal-rich population ([Fe/H] = +0.3) to a halo, metal-poor population ([Fe/H] = –0.8). Since the $b-y$ colors are sensitive to warm and hot stars blueward of the giant branch, changes in the horizontal branch immediately come to mind. Following the analysis from Peletier, Valentijn and Jameson (1 990), wc find that a composite Red and Blue HB contributing 5% of the total light at 5500Å will move the $b-y$ *colors* blueward by 0.044 mags from a RHB of a metal-rich population A pure 111111 population would move the $b-y$ colors blueward up to 0.1 mags. 'J'here is no impact on the near-IR colors and only a small shift in v – y. l'bus, wc conclude that all tile gradients in b – y, and some small amount of the gradients in v – y, are duc to the shifting contribution from BHB stars as the metallicity decreases into the halo. Detailed modeling using SED models combining the late stages of stellar evolution (HB and AGB populations) plus chemical evolution are yet to be developed, but these observations indicate that colors gradients will be an excellent test to the assumptions inherent in such modeling.

As mentioned above, many galaxies display a two component gradient characterized by a strong core gradient with a shallow halo gradient. This type of behavior is predicted by a hybrid merger plus a dissipation collapse scenario of galaxy formation where seed ellipticals formed at high redshift much along the lines of traditional dissipation processes with infalling, enriched gas producing the inner strong gradients. This scenario produces

a spectrum of ellipticals with masses ranging from dwarfs to approximately 1/2 L_*. Brighter elliptical where later constructed by mergers with neighbors, typically lower in luminosity and, thus, lower in mean metallicity. Outer gradients formed with the disruption and friction of accreting material to produce shallow gradients. Unfortunately, this scenario predicts that all the higher luminosity ellipticals all have double component gradients, which is not seen here. Other studies have suggested a merger history for bright elliptical based on kinematic or structural reasons (Schombert 1987), and perhaps an environmental effect is present where only cluster elliptical arc merger products.

Lastly, Figure 10 demonstrates the peculiar behavior of the color gradients with respect to the mean color of the galaxy. The near-IR colors and 6 — y show no trend; however, there is a positive correlation with the v — y gradients such that redder, more massive ellipticals have steeper v – y gradients. If wc continue our interpretation that v – y measures the light element abundance gradients, then this correlations indicates that the light to heavy element ratio changes with galaxy mass in a manner such that the light elements arc overenhanced in the cores. In the context of the differences with total light to heavy element changes with galaxy mass, then it appears that the light element enhancement is tied to the gravitational potential, i.e. light elements are stronger in the cores of galaxies and for higher mass systems. Several mechanisms are discussed in Worthey (1 992) for this type of enhancement, but only timescale difference in the rate of star formation are relevant to these observations, Overall, the basic mechanism is to somehow increase the number of Type 11 SN, which produce a majority of the light elements, but the cause remains outside the boundaries of these study.

V. Conclusions

We have presented a study of medium to bright ellipticals in six band passes from 3500Å to 2.2μm in order to quantify their colors and color gradients and to relate these to metallicity and properties of the underlying stellar population. Our choice of the Strömgren filter system allows us to introduce a ncw calibration to the Mg_2 system and [Fe/H] from our narrow band v – y indices, The long baseline from v to near-IR K allows a direct comparison of a spectral color versus a color dominated by the mean temperature of the giant branch (i.e. J - K). We summarize our observations and interpretation as the following:

(1) "1'here is a good correlation between v – y and Mg_2 providing a connection between one light element metallicity indicator (v – y centers on the CN blend) and another, Mg_2. A changing ratio of Mg/Fe in ellipticals (Worthey, Faber, and Gonzalez 1992) would be an annoying complication, but, not insurmountable with comparison to near-IR colors which measure the true metallicity, Z, as reflected in the changes in the temperature of cool giants due to opacity effects. If we adopt our $J-K$ colors as a measure of [Fe/II] and Worthey 's calibration to [Fe/H], then wc empirically determine that $d\mathrm{Mg_2}/d[\mathrm{Fe/H}] = 0.11$, which is lower than predicted by chemical evolution models.

(2) The color histograms can be found in Figure 4 corrected for Galactic extinction and redshift effects. Once the color-magnitude relation is taken into account, the dispersion is totally explained by observational error and color gradients supporting the idea that ellipticals arc a single generation family with minor modifications to account for duration of the initial burst of star formation and merger effects (see below),

(3) The color-magnitude relations for all five optical and near-IR colors arc shown in Figure 5. The strongest correlation exists for the metallicity colors, v -- y and $J - Ii'$. *When* $v - y$ is converted to [Fe/11] the implied mass-metallicity relation is $M \propto Z^{7.7}$. However, the near-IIL color, $J-K$ indicates a shallower mass-m metallicity relation of $M \propto Z^{4.6}$. We attribute this to a decoupling of light clement abundances to canonical measures such as [Fe/II] as proposed by Worthey, Faber and Gonzalez, It is worthwhile, in further studies, to specify comparison to indirect measures of Z, such as the Mg_2 system or the v — y CN colors presented herein, versus a direct measure of a galaxy's total metallicity from tile opacity of giants stars as reflected in the $J-K$ colors for this reveils clues to the style of star formation at formation time (i.e. an enhancement in Type 11 SN rates). We adopt the J — Ii' values as a measure of Z.

(4) The distribution of core metallicities ranges from [Fe/II] = –0.1 to + ().4 with a mean value of + 0.1. This value compares well with our own Galactic bulge metallicity of + ().3 (Rich 198(i). Halo metallicities arc around –-0.8, which is greater than our own Galaxy's halo or that of globular clusters around galaxies. The models of Arimoto and Yoshii (1986, see their Figure 3) predict an upper limit at [Fe/II] = 0.35, which is seen in the data.

(5) Gradients are present in every color for 13 of the 15 galaxies. The mean gradient in v– y is $\Delta(v-y)/\Delta\log r$ = –0.18 ± 0.08 or $\Delta(v-y)/\Delta\mu_V$ = –0.06 ± 0.03, expressed in the dimensionless units of surface brightness. This corresponds to $\Delta Mg_2/\Delta\log r$ = –0.044 ± 0.019 or $\Delta Mg_2/\Delta\mu$ = –0.015 ± 0.007. The gradients in the near-IR as just as significant, yet provide a different value of Δ[Fe/H]/$\Delta\log r$ = –0.44, a factor of two greater than the ones determined from optical band passes due to reasons discussed in (3), These are modest gradients with respect to the present models of galaxy formation (Fall and Efstathiou 1980, Fall and Rees 1985), but agree with previous values based on broad band colors, and with gradients determined from spectral features ($\Delta Mg_2/\Delta\log r$ = –0.058 ± 0.027, Gorgas, Efstathiou and Salamanca 1990).

(7) The color-gradient correlation in Figure 10 shows that more massive galaxies have steep gradients. Since gradient strength is an indicator of the timescale of the initial phase of star formation, this supports the hypothesis that high mass galaxies had a faster epoch of star formation than less massive galaxies. Deconvolving narrow band colors and stellar population effects (as they affect M/L) should allow a detailed understanding of the [Fe/H] by mass within a galaxy, This would yield a powerful tool in the modeling of the galaxy evolution and constraining initial conditions of galaxy formation.

(8 A double component nature to the color gradients is found in many of the ellipticals studied herein, both in the optical and near-IR. These two components are always represented by a strong core gradient and a shallow halo gradient (see also Thomsen and Baum). This behavior is consistent with a formation scenario where seed cores are formed by disspational star formation with a later epoch of mergers with metal-poor neighbors (see below). At the very least, this real variations in radial gradients implies a complicated formation process.

(9) The surprising behavior of our continuum color, b – y indicates that changes in stellar population forbid a simple analysis of metallicity without guidance by SED models. Galaxies with gradients in v – y also display weak gradients in b – y and, despite an expected factor of ten less sensitivity, the b – y gradients are only a factor of two less than the v — y gradients, Our interpretation of this phenomena is based on the contribution from BHB stars as the mean metallicity of tile underlying stellar population moves from a [l'e/II] value of +0.3 in the core to -0.8 in the halo. Our crude estimates based on a 1% contribution at 5500Å suggests that population difference can explain all of the b – y gradients. This serves as a cautionary tale for future multi-color photometry studies.

Our basic conclusions differ little from Thomsen and Baum (1 989) in that we find elliptical are primarily high [Fe/11] systems with low gradients. Clearly, these gradients represent, a scenario where metal-poor stars can be found at all radii, but more metal-rich stars tend to form later and are more centrally concentrated. We also find that halo stars in disk galaxies are not as metal-rich as the halo stars in elliptical or their orbiting globular clusters. Note that the above conclusion indicate that elliptical arc not composed of distinct stellar population components like our Galaxy (i.e. thin disk, thick disk, bulge and halo), but rather contains a smooth continuum of stars all formed within approximately 1 Gyr during the epoch of initial star formation. Ellipticals are, to first order, well matched to a simple, single metallicity model in their integrated properties, but as the gradients in this study shows, there is a much more complex nature to the underlying stellar population that is resolved in a spatial manner. This has farther reaching implications for different wavelengths, due to complications from BHB stars, for a metal-poor population may have a negligible effect on optical bandpasses, yet will be substantial in the near and far-UV portions of the spectrum,

It is not surprising to find, as we learn more about the composition of ellipticals, that the early star formation history appears more complicated than the standard scenarios of galaxy formation. The two component gradients structure that we find implies two possible scenarios for elliptical formation. One is that there existed an early phase of star formation which was slower than the timescales for gas infall until a mean [Fe/H] of – 1 was reached. 'J'hen, cooling through metal lines increased the mean SFR which then sharpened the inner gradients. The second scenario is based on the idea that if the subunits that build protogalaxies are stellar then the metallicity gradients are weak, If those subunits are gas-rich, then strong gradients are produced (Fall and Rees 1985). So that our observations support the idea that the core region of ellipticals arc the original seeds build from gaseous protogalactic lumps. And the halo regions, and a substantial amount of the mass, is produced by mergers of neighboring protogalaxies after the first phase of star formation. This is also supported by structural and kinematic arguments for bright ellipticals (Schombert 1987), although it must be remembered that we have not exhausted different ideas to produce varying gradients in color. For example, stochastic variation in the

initial star formation weakens gradients in high σ systems. Finally, wc note that the lack of an extreme metal-poor population in the halo of elliptical also supports the theory of rapid enrichment due to the strength of the initial phase of star formation. lhis era of strong star formation also quickly built a hot thermal gas component, seen at the current epoch as an X-ray halo. This halo could also serve to prevent the formation of [Fe/11] < –1 stars from remaining pockets of metal-poor gas or infalling gas preserving the gradients we see today.

The authors wish to acknowledge the generous allocation and support of the telescopes at MDM and KPNO. We also wish to thank D. Silva, R. Elston and J. Salzer for enlightment on the reduction of I RIM data, 'I'. von Hippel for taking some of the data used herein and M. Merrill and R. Probst for assistance at the telescope. G. Bothun's unpublished preprint was of enormous help in distinguishing what science could be extracted from the current generation of IR arrays and R. Pildis for insight. The NASA/IPAC Extragalactic Database (NED) is operated by the Jet Propulsion Laboratory, California Institute of '1'ethnology, under contract with the National Aeronautics and Space Administration.

References

van Albada, T.S. 1982, *M. N. R. A. S., 201,939.*

Arimoto, N. and Yoshii, Y. 1986, *A. A.,* **164**, *260.*

Bell, R., Hesser, J. and Cannon, R. 1983, *Ap. J.*, 269, 580.

Bothun, G. 1990, preprint.

Bothun, G. and Gregg, M. 1990, *Ap. J.*, **350**, 73.

Boroson, T.A. and Thompson, 1.11.1983, *A. J.*, 92, 33.

Bruzual, G. 1983, *Ap. J.*, 273, 105.

Burstein, D. 1985, *P. A. S. P.*, 97, 89.

Burstein, D., Bertola, F., Buson, I,., Faber, S. and Lauer, 1'.1988, *Ap. J.*, 328, 440.

Buzzoni, A., Gariboldi, G. and Mantegazza, I,. 1992, *A. J.*, 103, 1814.

Carlberg, R. 1984, *Ap. J., 286, 403.*

Carney, B. 1988, in *IA U Symposium 126, The Harlow-Shapley Symposium 011 Globular (luster Systems in Galaxies,* cd. J. Grindlay and A. Davis Philip (Dordrecht: Reidel), p. 133.

Cohen, J.G. 1986, *A. J.*, 92, 1039.

Davidage, '1'., 1992, *A. J., 103, 1512.*

Davis, L., Cawson, M., Davies, R. and Illingworth, G. 1985, *A. J., 90, 169.*

Dressler, A., Lyden-Bell, l)., Burstein, D., Davies, R., Faber, S., Terlevich, R. and Wegner, G. 1987, *Ap. J., 313, 42.*

Elias, J., Frogel, J., Matthews, I{. and Neugebauer, G. 1982, *A. J., 87,* 1029.

Faber, S., Burstein, D. and Dressier, A. 1977, *A. J., 82, 941.*

Faber, S. and Gallagher, J. 1979, *Ann. Rev. Astron. Astrophys.*, 17, 135.

Faber, S., Wegner, G., Burstein, D., Davies, R., Dressler, A,, Lyden-Bell, D. and Terlevich, R. 1989, *Ap. J. Suppl., 69,763.*

Fall, S. and Efstathiou, G. 1980, *M.N.R.A.S.*, 193, 189.

Fall, S. and Rees, M. 1985, *Ap. J., 298, 18.*

Franx, M. and Illingworth, G. 1990, *Ap. J., 359, 1,41.*

Frogel, J.A., Persson, S. E., Aaronson, M. and Matthews, K. 1978, *Ap. J., 22o, 75.*

Gott, J.R. and Thuan, 'l'.X. 1976, *Ap. J., 204, 649.*

Gorgas, J., Efstathiou, G. and Salamanca, A. 1990, *M. N.R. A. S., 245, 217,*

Griersmith, D. 1982, *A. J., 87, 462.*

Guiderdoni, R. and Rocca-Volmerange, B. 1987, *A. A.,* **186**, *1,*

Hamilton, D. 1985, *Ap. J., 297, 371.*

Helou, G., Madore, B., Schmitz, M., Bicay, M., wu, X. and Bennett, J.]99], *Databases and On-Line Data in Astronomy,* ed. 1). Egret and M. Albrecht (Dordrecht: Kluwer), p. 89.

Jedrzejewski, R. 1987, *M.N.R.A.S.*, **226**, *747.*

Larson, R.B. 1975, *M. N. R. A. S.*, 173, 671.
Michaud, R. 1980, *A. A., 91, 122.*
Peletier, R., Davies, R., Illingworth, G., Davis, L. and Cawson, M. 1990, *A. J., 100,* 1091.
Peletier, R., Valentijn, E. and Jameson, R. 1990, *A. A., 233, 62.*
Perry, C., Olsen, E. and Crawford, D. 1987, *P. A. S.P.*, 99, 1184.
Persson, S., Frogel, J. and Aaronson, M. 1979, *Ap. J. Suppl., 39, 61.*
Rakes, K., Schombert, J. and Kreidl, T. 1991, *Ap. J., 377, 382,*
Rakos, K. and Schombert, J.M. 1993, in prep.
Rich, R, 1988, *A. J., 95, 828.*
Rose, J. 1985, A. J., 90, 1927.
Sandage, A. and Visvanathan, N. 1978, *Ap. J., 223, 707.*
Schneider, D., Gunn, J. and Hoessel, J. 1983, *Ap. J.*, 264, 337.
Schombert, J. 1987, *Ap. J. Suppl., 64, 643.*
Schombert, J., West, M., Zucker, J. and Struble, M. 1989, *A. J., 98,* 1999.
Schombert, J., Hanlan, P. and Barsony, M. 1993, in prep.
Silva, D. and Elston, R. 1992, preprint.
Spinrad, 11.1986, *P. A. S. P., 98, 269.*
Strom, S. E., Strom, K. M., Goad, J. W., Vrba, F.J. and Rice, W. 1976, *Ap. J., 204, 684.*
Stiavelli, M. and Matteucci, F. 1991, *Ap. J., 377, 1,79.*
Thuan, T. and Puschell, J. 1989, *Ap. J., 347, 214.*
Thomsen, B. and Baum, W.A. 1989, *Ap. J., 347, 214.*
Tinsley, B.M. 1980, *Fund. of Cosmic Physics*, 5, *287.*
de Vaucouleurs, G. and de Vaucouleurs, A. 1972, *Mem. R. Astron. Sot., 77, 1.*
Visvanathan, N. and Sandage, A. 1977, *Ap. J., 216, 214.*
White, S.D.M. 1980, *M. N. R. A. S.*, **191**, 1P.
Worthey, G., 1992, Ph.D. Thesis, Univ. of Calif., Santa Cruz.
Worthey, G., Faber, S.M. and Gonzalez, J.J. 1992, *Ap. J, 398,* 69.
Wyse, R. 1985, *Ap. J., 299, 593.*

'1'able 1. Photometric Properties

Object	MB	$u-v$	$u-y$	$v-y$	$b-y$	$v-y_o$	V-I	$J-K$	Mg_2
N315	-21.6	1.39	2.87	1.48	0.63	1.47	3.37	0.94	0.283
N41O	–21.3	1.27	2.85	1.57	0.66	1.58	3.41	0.93	...
N507	–21.3	1.33	2.83	1.50	0.69	1.51	3.42	0.86	0.302
N631	–19.6	1.40	2,96	1.56	0.68	1.58	. . . . .		...
N680	–19.8	1.22	2.74	1.53	0.69	1.53	3.16	0.83	0.287
N2693	–20.5	1.10	2.78	1.68	0,66	1.74	3.26	0.87	0.328
N2974	–19.2	1.14	2.76	1.62	0.69	1.66	3.40	0.88	0.300
N3608	–18.5	1.19	2.78	1.60	0.68	1.62	3.24	0.83	0.312
N3998	–18.5	1.03	2.80	1.77	0.63	1.67	. . . . .		...
N4261	–20.3	1.20	2.82	1.62	0.66	1.64	3.26	0.89	0.330
N4374	–20.4	1.17	2.83	1.66	0.69	1.67	3.32	0.82	0.305
N4406	–20.6	1.23	2.92	1.69	0.58	1.71	. . . . .		0.311
N4477	–19.0	1.17	2.79	1,63	0.70	1.64	3.37	0.86	
N5846	–20,3	1.19	2.84	1.65	0.61	1.65	. . . . .		0.321
N6278	–19.0	1.31	2.82	1.51	0.59	1.47	. .		...
N6411	–20.2	1.31	2.80	1.49	0,68	1.55	. . . .		0.270
N6495	–19.3	1.26	2.79	1.53	0.66	1.54	. . .		
N6702	–20.4	1.30	2.79	1.49	0.69	1.50	3.15	0.84	0,272
N6703	–19.9	1.25	2.78	1.53	0.69	1.60	3.28	0.81	0.280
N7332	–18.7	1,32	2.77	1.44	0.67	1.45	3.02	0.80	...
N7562	–20.1	1.14	2.61	1.47	0.62	1.52	3.33	0.92	0.291
N7626	–20.7	1.17	2.94	1.80	0.75	1.75	. . . . .		0.336
N7785	–20.5	1.31	2.90	1.59	0.75	1.61	3.20	0.86	0.296

Table 2. M can colors

$< u - v >= 1.23 \pm 0.09$
$< u - y >= 2.82 \pm 0.06$
$< v - y >= 1.59 \pm 0.09$
$< b - y >= 0.67 \pm 0.04$
< Fe/H >= -t 0.03

Table 3. Color Gradients

Object	$\frac{\Delta(v-y)}{\Delta \log r}$	$\frac{\Delta(V-K)}{\Delta \log r}$	$\frac{\Delta(J-K)}{\Delta \log r}$
N315	-0.12 ± 0.01	-0.13 ± 0.04	-0.07 ± 0.04
N41O	-0.16 ± 0.02	-0.38 ± 0.04	-0.07 ± 0.04
N507	-0.09 ± 0.01	-0.51 ± 0.03	-0.30 ± 0.08
N631	-0.19 ± 0.04	. . .	...
N680	-0.13 ± 0.02	-0.41 ± 0.05	-0.23 ± 0.05
N2693	-0.43 ± 0.09	-0.24 ± 0.08	-0.17 ± 0.05
N2974	-0.29 ± 0.03	-0.23 ± 0.02	-0.08 ± 0.03
N3608	-0.25 ± 0.05	-0.30 ± 0.08	-0.08 ± 0.04
N3998	-0.25 ± 0.02	. . .	.
N4261	-0.20 ± 0.04	$-0.2 : \pm 0.10$	-0.05 ± 0.09
N4374	-0.20 ± 0.01	-0.18 ± 0.01	-0.12 ± 0.01
N4406	-0.21 ± 0.01	. . .	...
N4477	-0.15 ± 0.02	-0.21 ± 0.01	-0.12 ± 0.01
N5846	$-0.104. 0.01$	. . .	
N6411	-0.12 ± 0.02	. . .	...
N6495	-0.13 ± 0.03	. . .	...
N6702	-0.08 ± 0.01	-0.34 ± 0.06	-0.17 ± 0.06
N6703	-0.15 ± 0.06	.	
N7332	$-0.16 \pm 0,01$	-0.38 ± 0.05	-0.16 ± 0.04
N7562	-0.23 ± 0.02	-0.04 ± 0.08	-0.03 ± 0.05
N7626	-0.27 ± 0.01	. . .	...
N7785	-0.14 ± 0.02	-0.21 ± 0.05	$--0.25+ 0.05$

Figure Captions

Figure 1 - The Strömgren and near-IR filter systems shown together with a spect rum of a typical bright elliptical. Broad spectral features arc marked. Note, in particular, the v filter lies in a region dominated by the 4170Å CN blend. The near-IR filters J HK arc identical to those described in Persson, Frogel and Aaronson (1979).

Figure 2- Core v – y colors versus the Mg_2 index. The Strömgren color v – y can be calibrated to the Mg_2 metallicity system (Faber *et al.* 1989) as shown in this linear fit to the correlation. The fit parameters arc listed. Closed symbols represent normal elliptical) whereas open symbols represent ellipticals with bright X-ray halos or cooling flows.

Figure 3- Comparison of Mg_2 indices and v – y colors (converted to Mg_2) for NGC 2693. Mg_2 line measurements are from Davidage (1 992) with his error bars shown. 'J'here is excellent agreement between the two methods supporting our conclusion that measurements from $v-y$ can be mapped onto the Mg_2 system.

Figure 4- Luminosity weighted integrated colors for the sample in all optical and near-IIt filters. Colors are uncorrected for the color-magnitude relation. If corrected, the dispersions are purely observational error. '1'here was no significant separation between normal and cooling flow galaxies in the optical passbands; however, differences in the near-lli (not shown) will be discussed in a future paper.

Figure 5 - The color-magnitude relation for three optical and two near-l R colors. Blue magnitudes arc taken from the literature. '1'here are solid correlations in all colors but the continuum color, $b-y$. The mass-metallic.ity relations implied by these correlations arc inconsistent, between the optical and near-IR. The most likely candidate for this inconsistent behavior is a breakdown in the optical, main sequence, light element indicators of Z and the near-IR giant branch indicators. As in previous figures, normal versus cooling flow ellipticals arc marked with different symbols.

Figure 6- Color profiles in the optical metallicity color, $v - y$. Gradient values are found in Table 1. Error bars are assigned from RMS errors on the surface photometry. Upward arrows indicate the region of the profile which were fit for the gradients listed in Table 3.

Figure 7- Color profiles in the cross-band color, $V - K$. Gradient values are found in g'able 1. Error bars are assigned from RMS errors on the surface photometry. Upward arrows indicat e the region of the profile which were fit for the gradients listed in Table 3.

Figure 8 - Color profiles in the near-IR color, $J - K$. Gradient values arc found in Table 1. Error bars are assigned from RMS errors on the surface photometry. Upward arrows indicate the region of the profile which were fit for the gradients listed in Table 3.

Figure 9- Color profiles of NGC 6703 and NGC 7626 plotted versus V surface brightness as pcr the prescription of Thomsen and Baum. These two galaxies exhibit the double component nature of steep inner gradients and weak outer gradients discussed in text.

Figure 0 - Color gradients versus mean integrated colors. The metallicity color, v – y shows a correlation with gradient slope (in mags per log r). The $b - y$ colors displys no correlation and the J — K color exhibits a weak and opposite correlation to the v — y colors,

Figure 1 - Core and halo [Fe/H] values assigned from the v – y colors and the conversion formula in §IIc. Halo values arc determined at r_e, the half-light radius from $r^{1/4}$ fits. The mean *Core* value *is* +0.3, but the halo metallicities are much higher than globular clusters at similar radii.

Mary Barsony: Harvard-Smithsonian Center for Astrophysics, 60 Garden St., MS 63, Cambridge, MA 02138

Patricia Hanlan: Dept. of Astronomy, Univ. of Michigan, Ann Arbor, MI 48109

Karl Rakes: Institute for Astronomy, Turkenschanzstrasse 17, A-1 180, Wien, Austria

James M. Schombert: IPAC/Caltech, MS 100-22, Pasadena, CA 91125

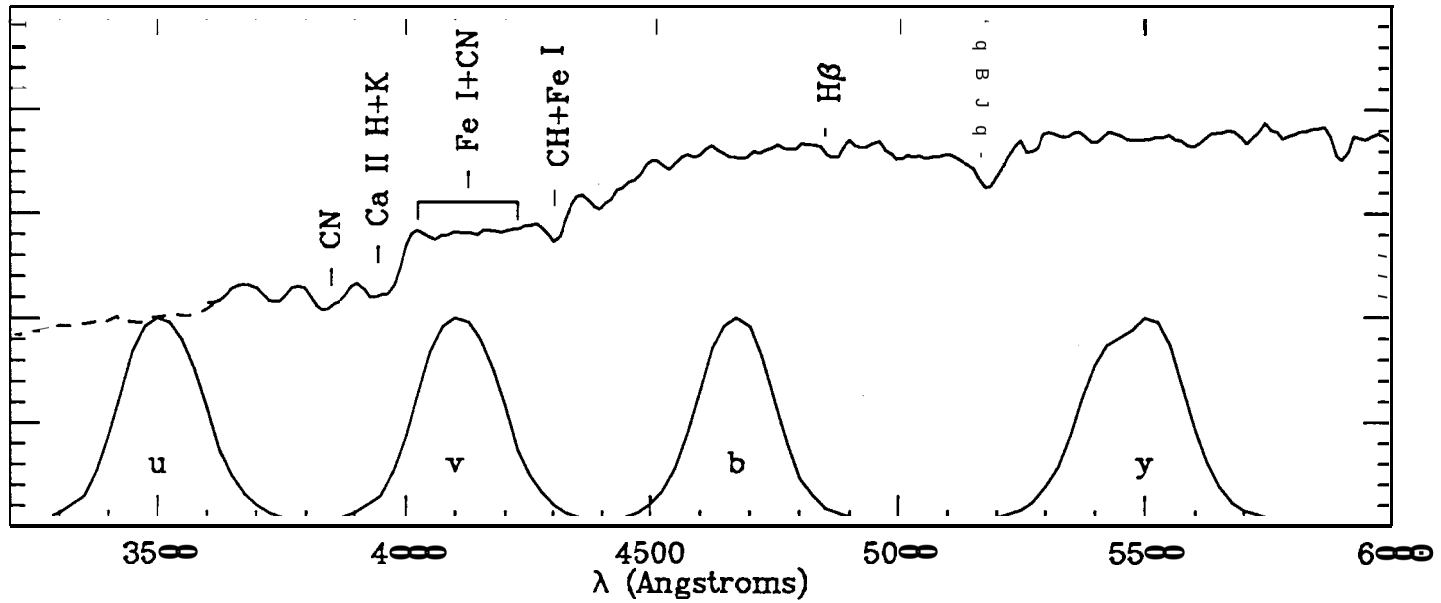
CN
Ca II H+K
Fe I+CN
CH+Fe I
Hβ
b
a
u
v
b
y
3500
4000
4500
5000
5500
6000
λ (Angstroms)

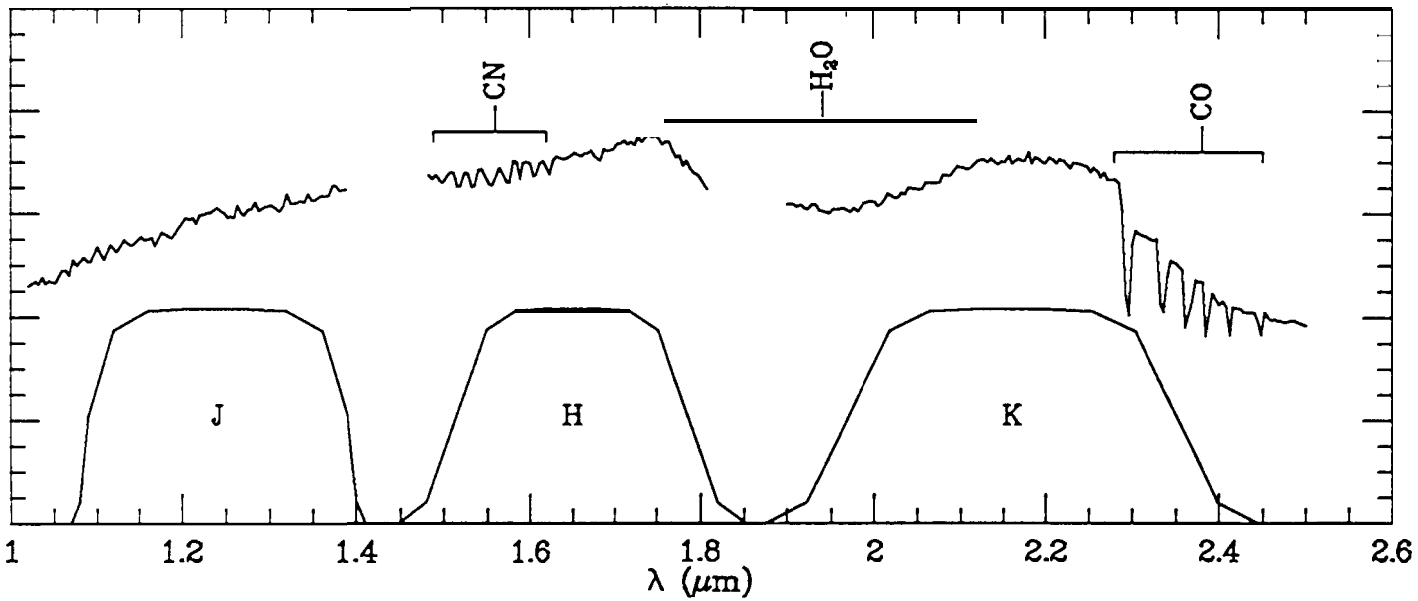
CN
H2O
CO
J
H
K
1
1.2
1.4
1.6
1.8
2
2.2
2.4
2.6
λ (μm)

Figure 1

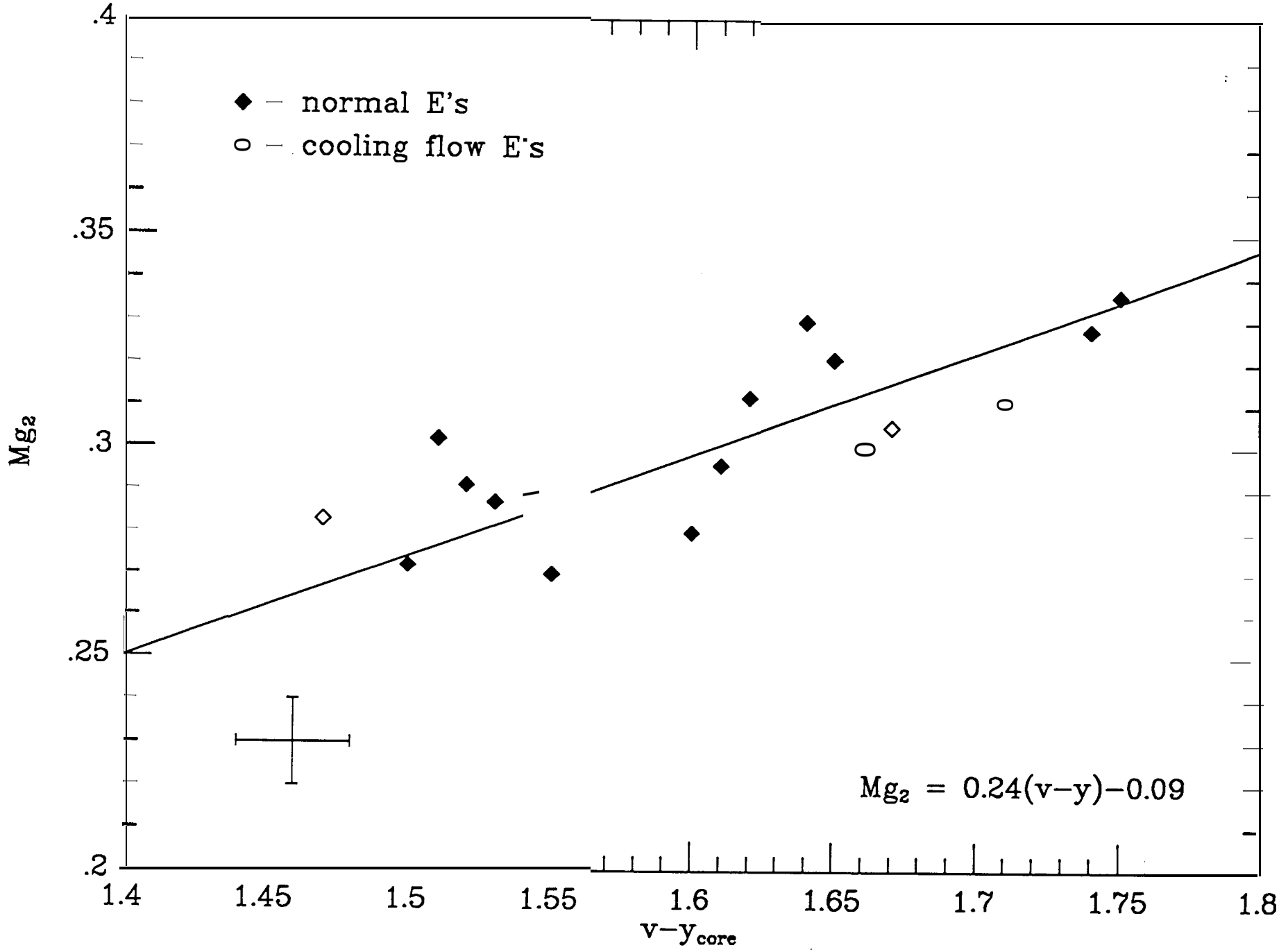
.4
.35
.3
.25
.2
Mg2
◆ – normal E's
o – cooling flow E's
Mg2 = 0.24(v−y)−0.09
1.4
1.45
1.5
1.55
1.6
1.65
1.7
1.75
1.8
v−ycore

Figure 2

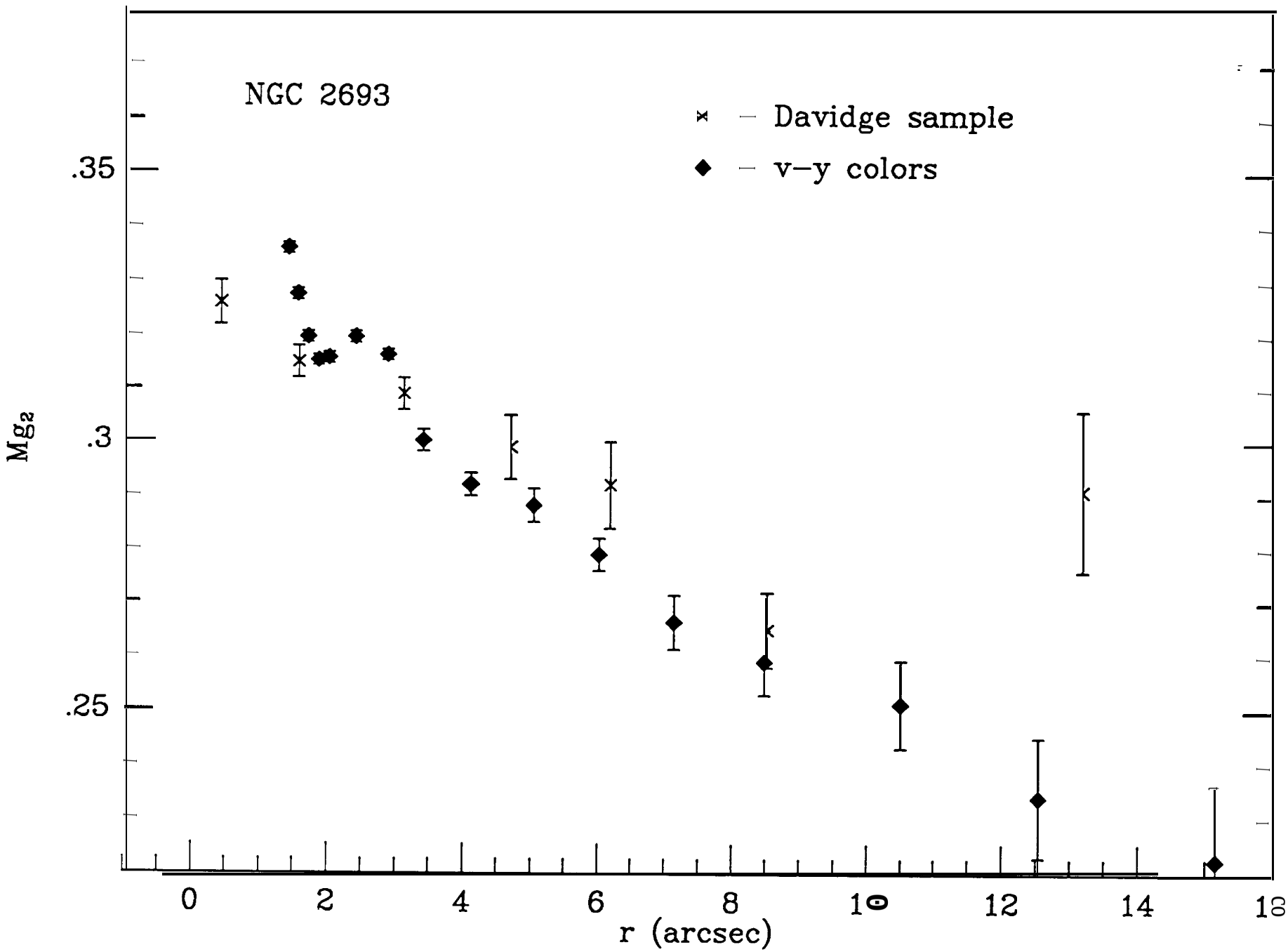
NGC 2693
× – Davidge sample
◆ – v–y colors
.35
.3
.25
Mg_2
0
2
4
6
8
10
12
14
18
r (arcsec)

Figure 3

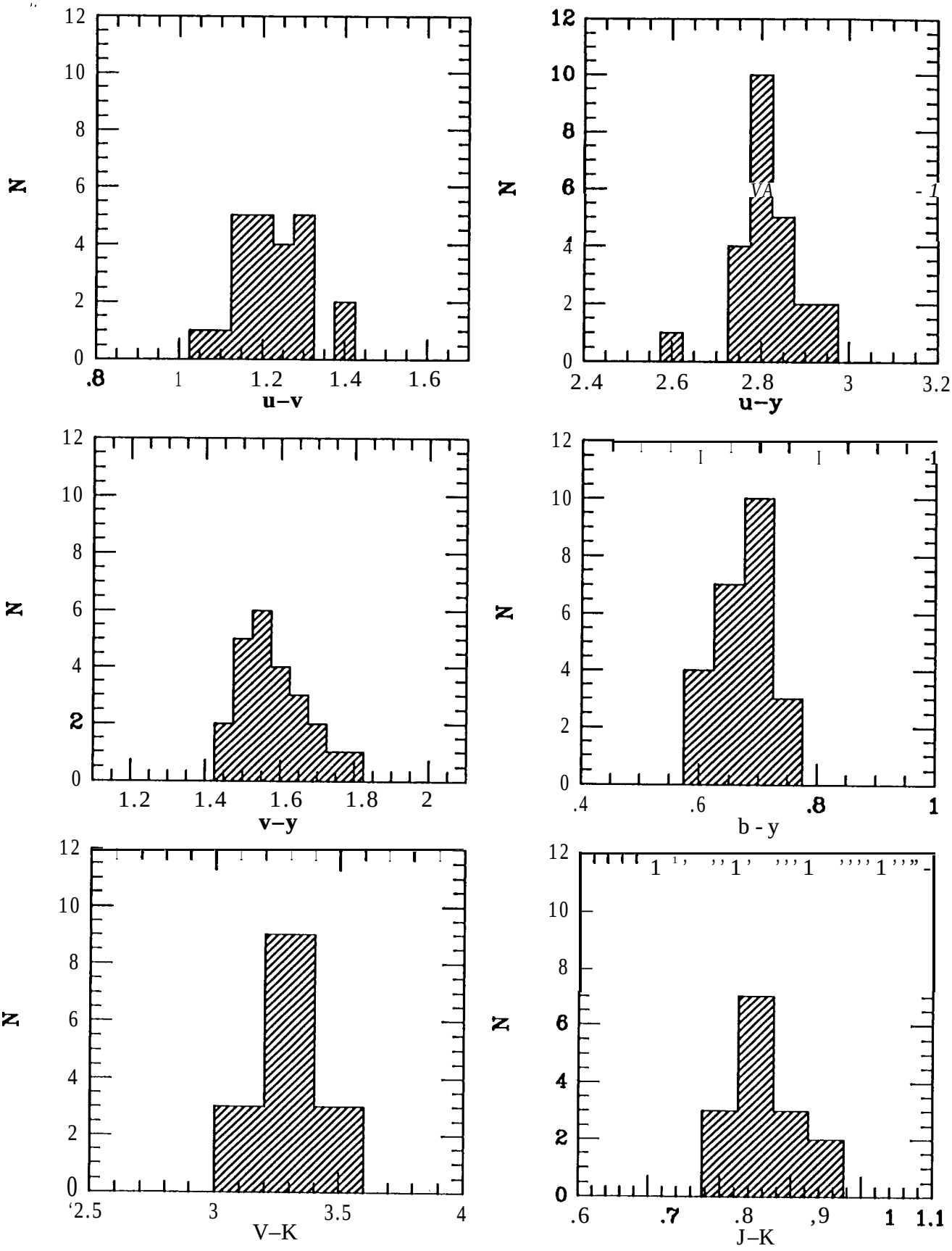

Figure 4

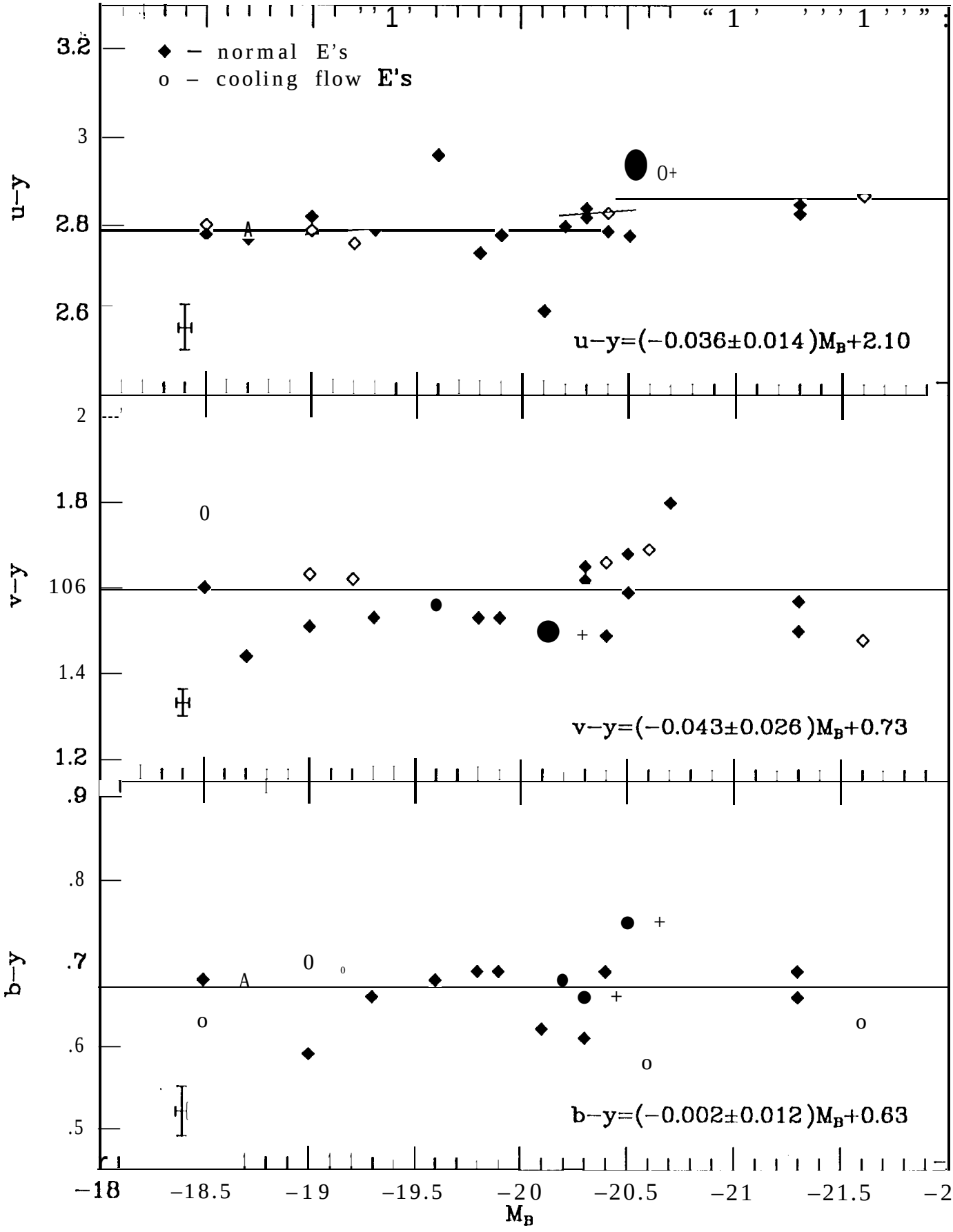
◆ – normal E's
o – cooling flow E's
u–y
v–y
b–y
u–y=(–0.036±0.014)M_B+2.10
v–y=(–0.043±0.026)M_B+0.73
b–y=(–0.002±0.012)M_B+0.63
M_B
3.2
3
2.8
2.6
2
1.8
1.06
1.4
1.2
.9
.8
.7
.6
.5
–18
–18.5
–19
–19.5
–20
–20.5
–21
–21.5
–22

Figure 5

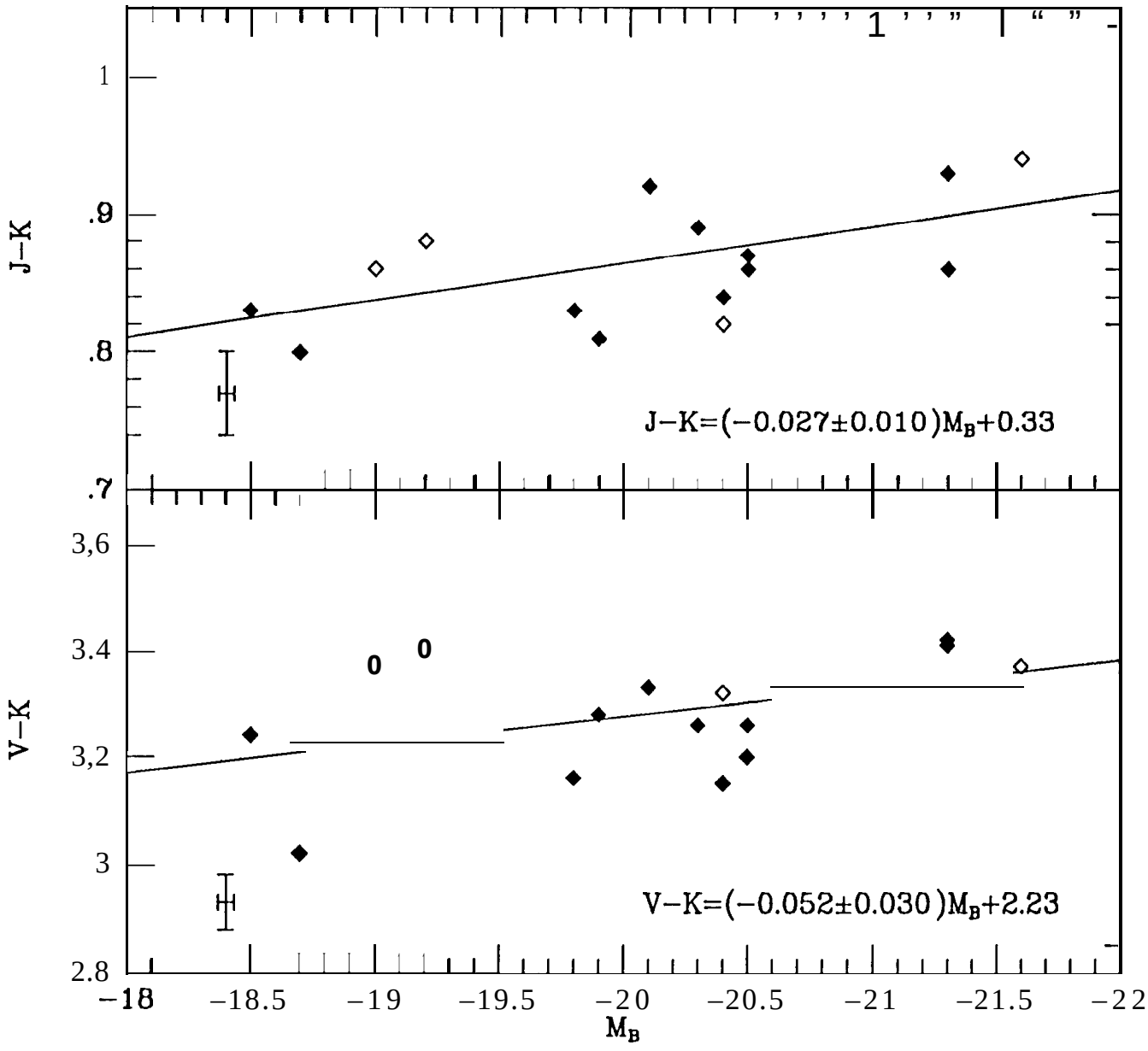

Figure 5 (cont.)

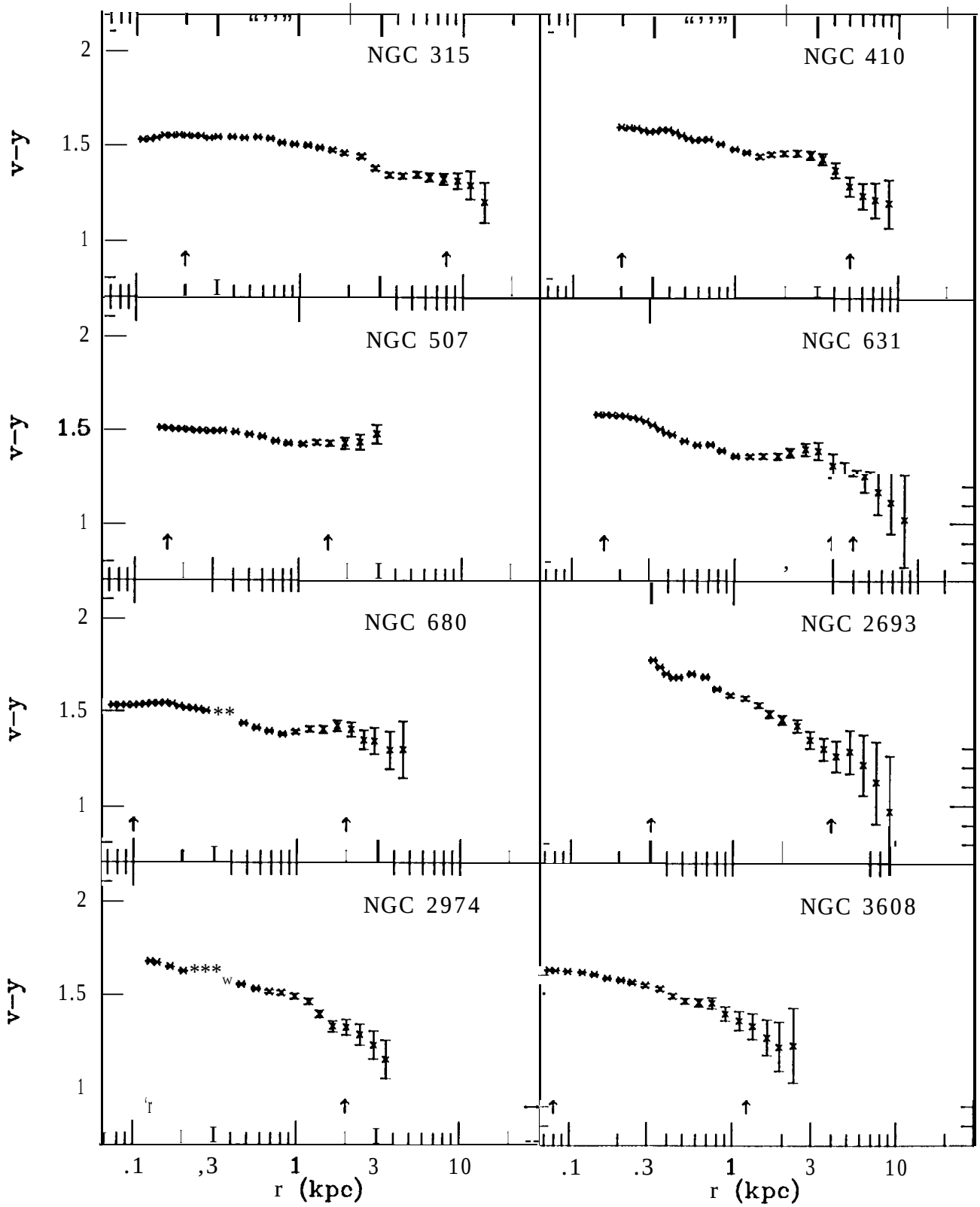
NGC 315
NGC 410
NGC 507
NGC 631
NGC 680
NGC 2693
NGC 2974
NGC 3608
v–y
r (kpc)
.1
.3
1
3
10

Figure 6

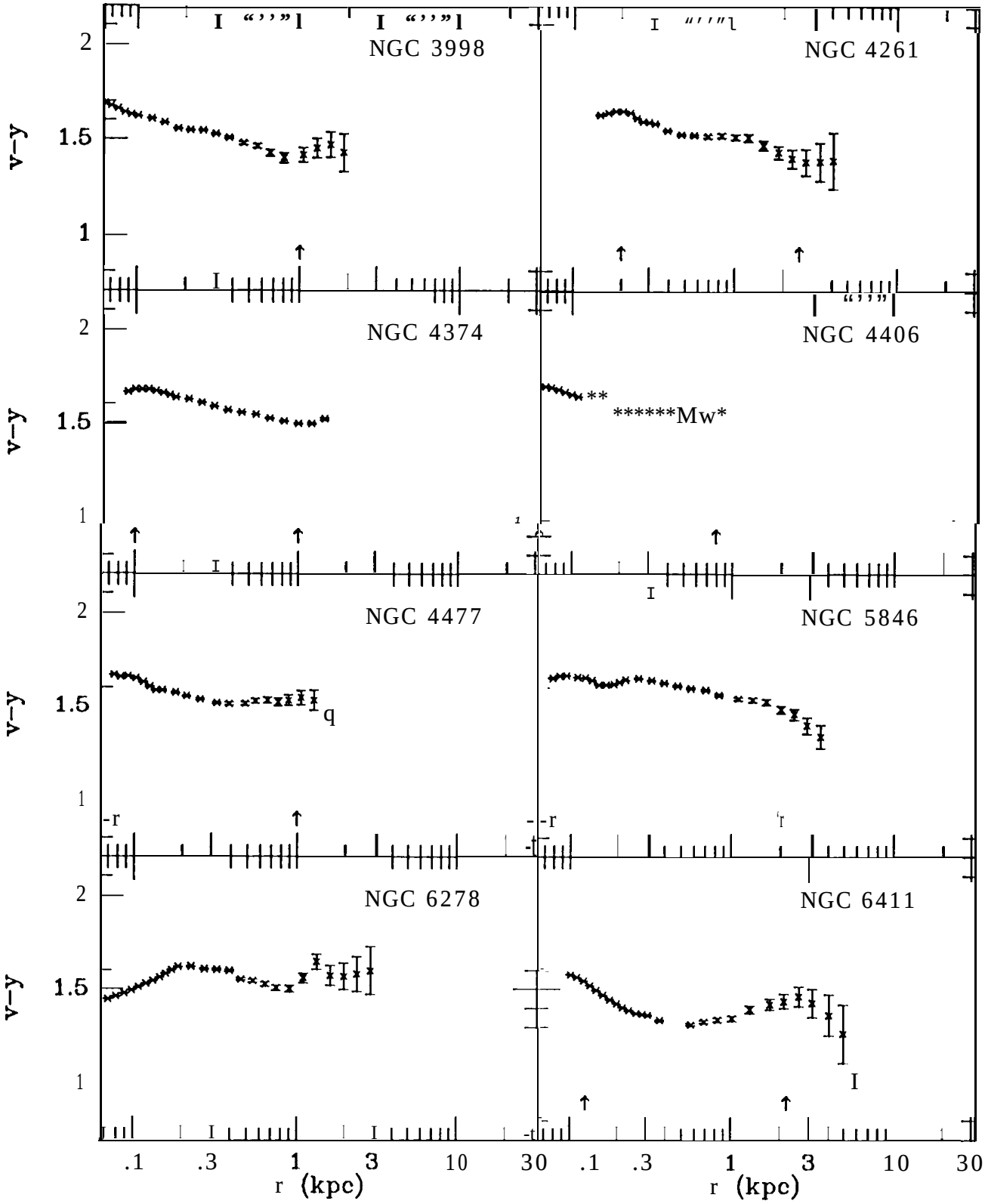

Figure 6 (cont.)

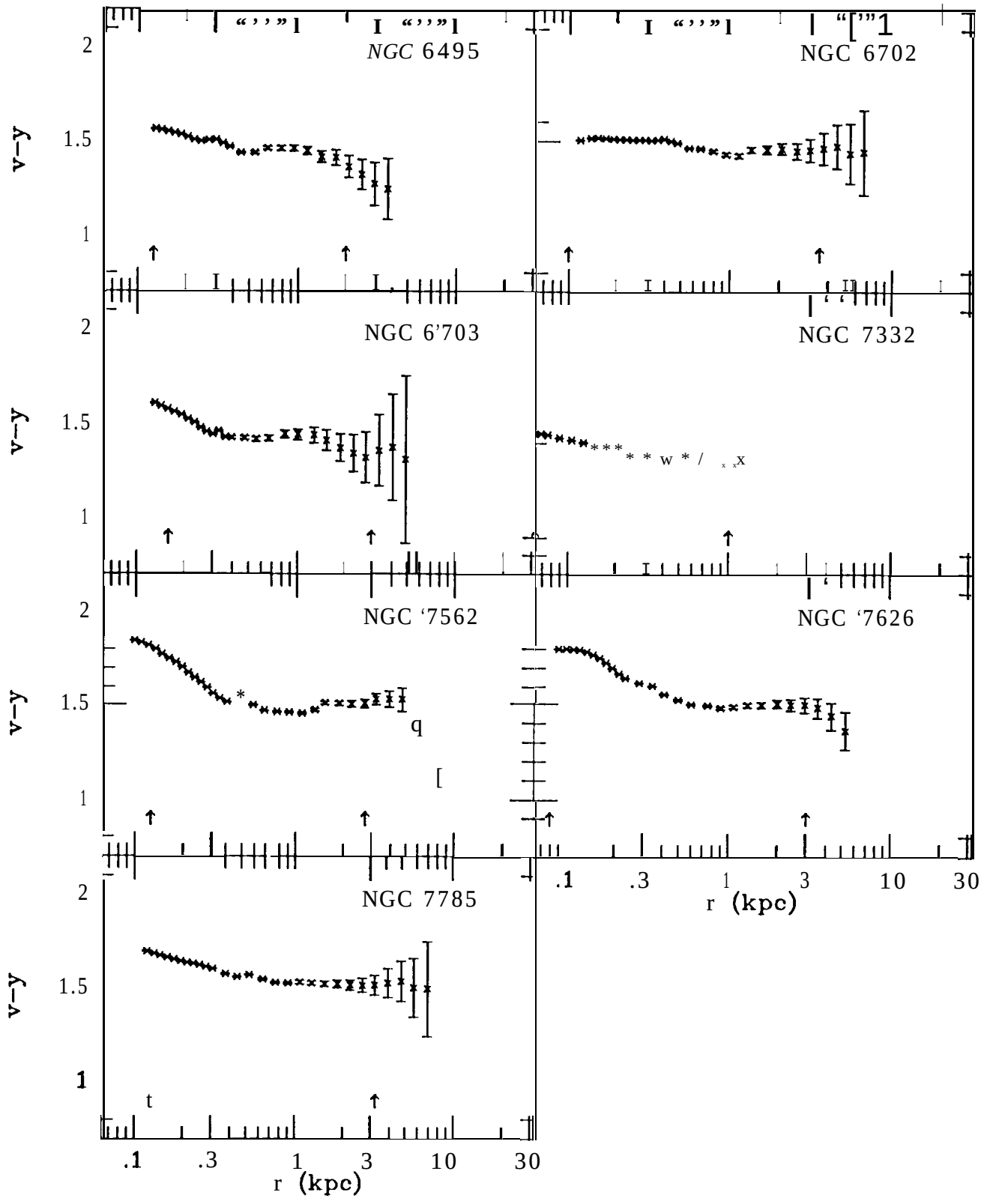

Figure 6 (cont.)

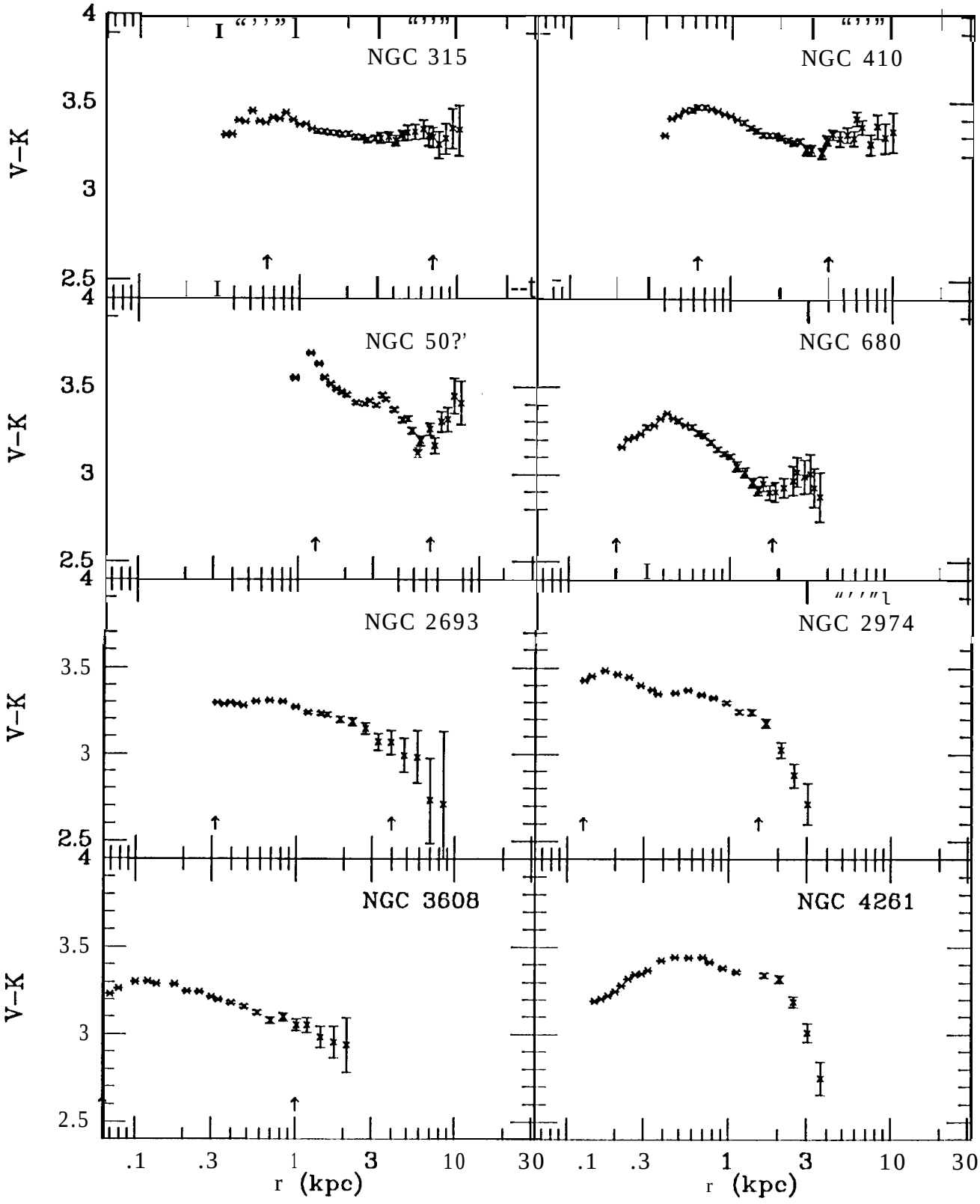
NGC 315
NGC 410
NGC 50?'
NGC 680
NGC 2693
NGC 2974
NGC 3608
NGC 4261
V-K
r (kpc)
.1
.3
1
3
10
30

Figure 7

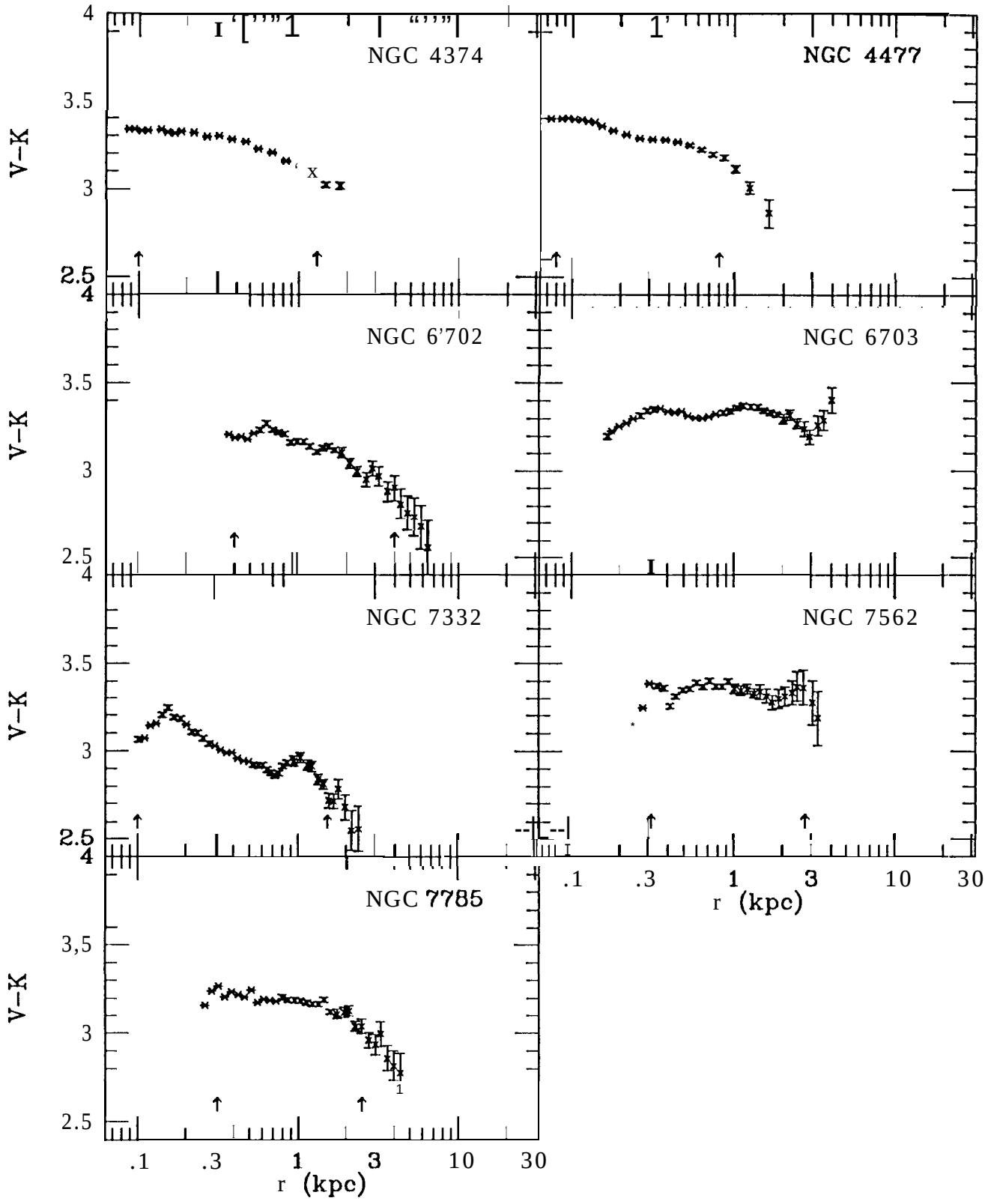

Figure 7 (cont.)

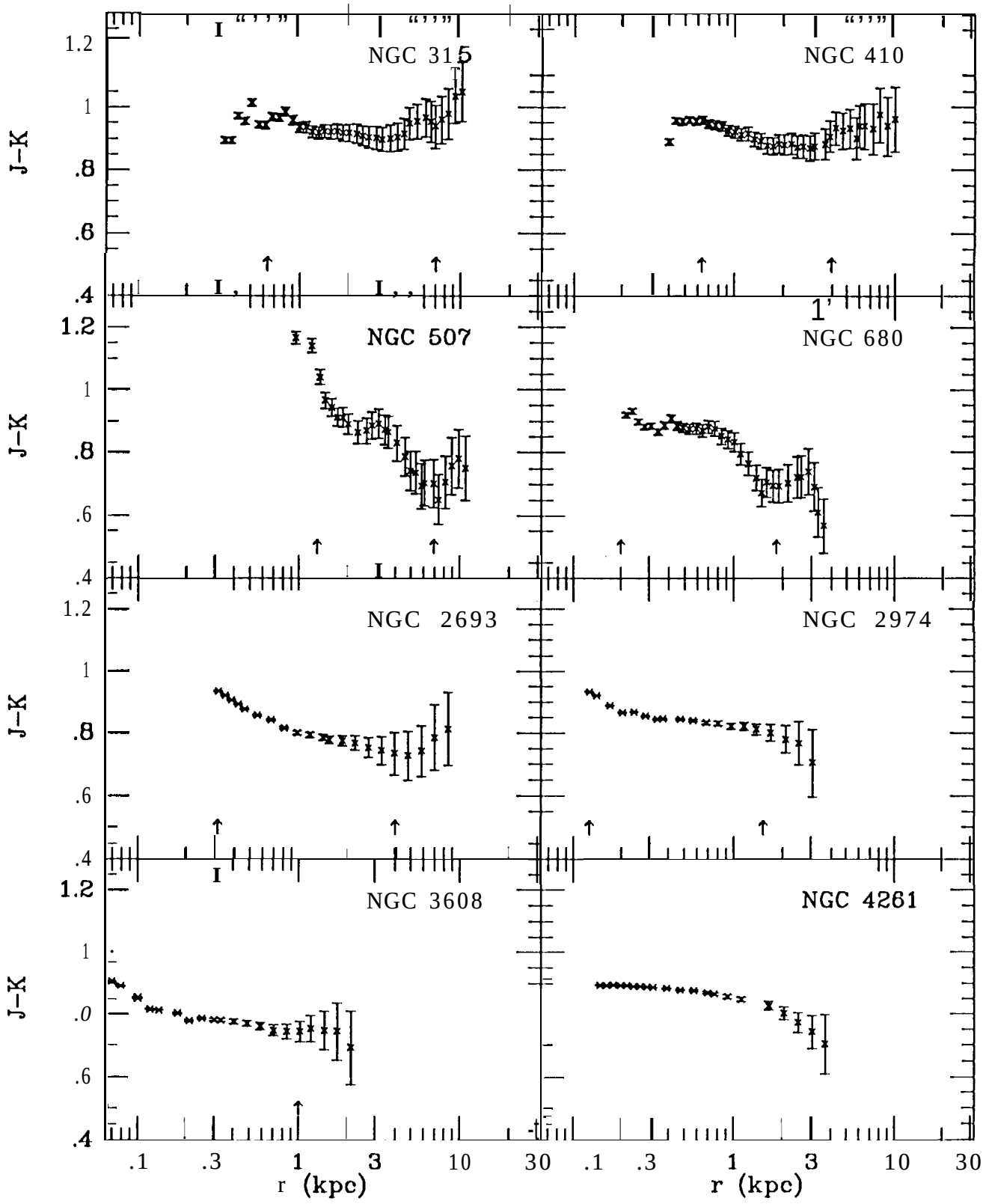
NGC 315
NGC 410
NGC 507
NGC 680
NGC 2693
NGC 2974
NGC 3608
NGC 4261
J-K
1.2
1
.8
.6
.4
.0
.1
.3
1
3
10
30
r (kpc)
1'

Figure 8

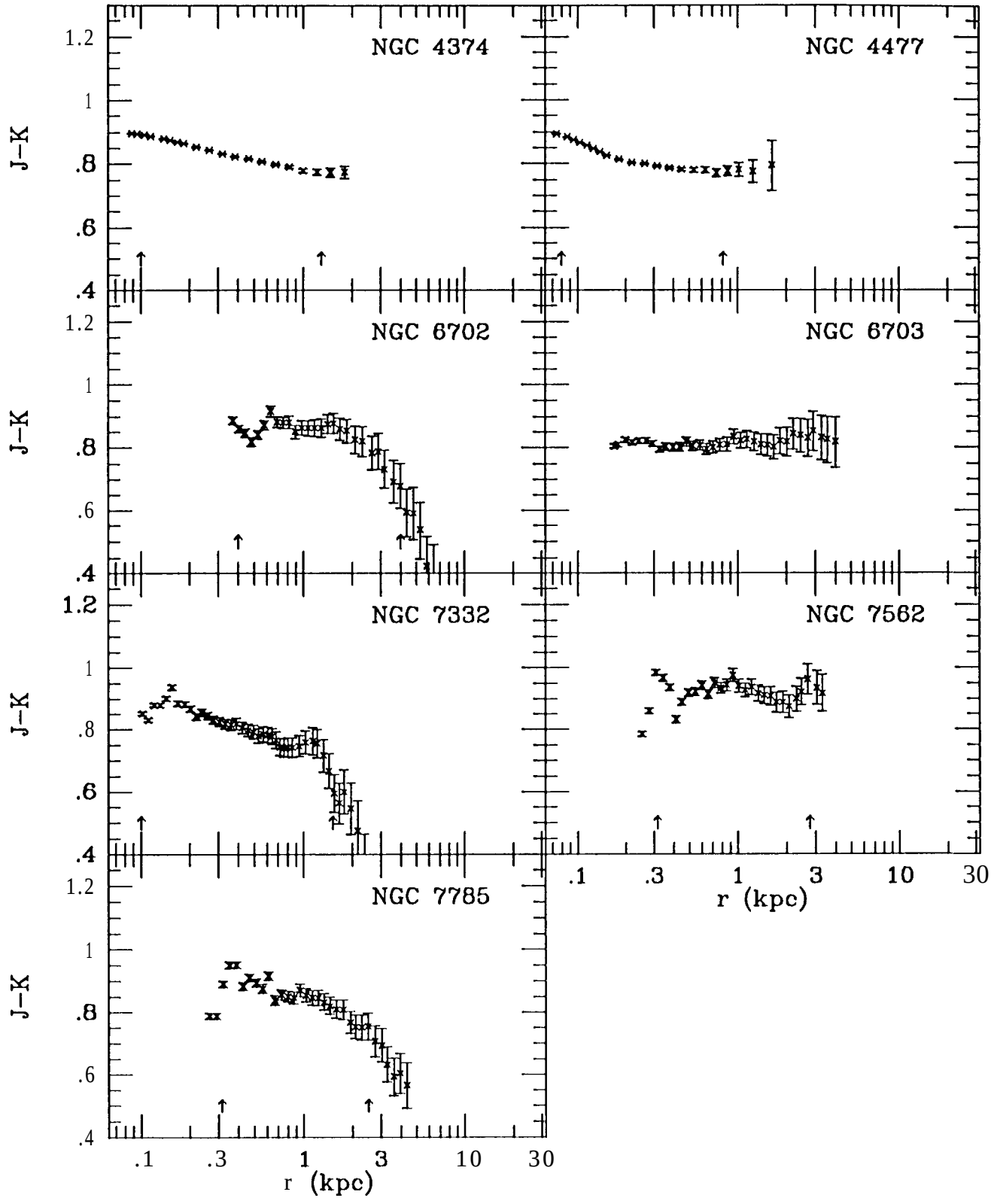

Figure *8* (cont.)

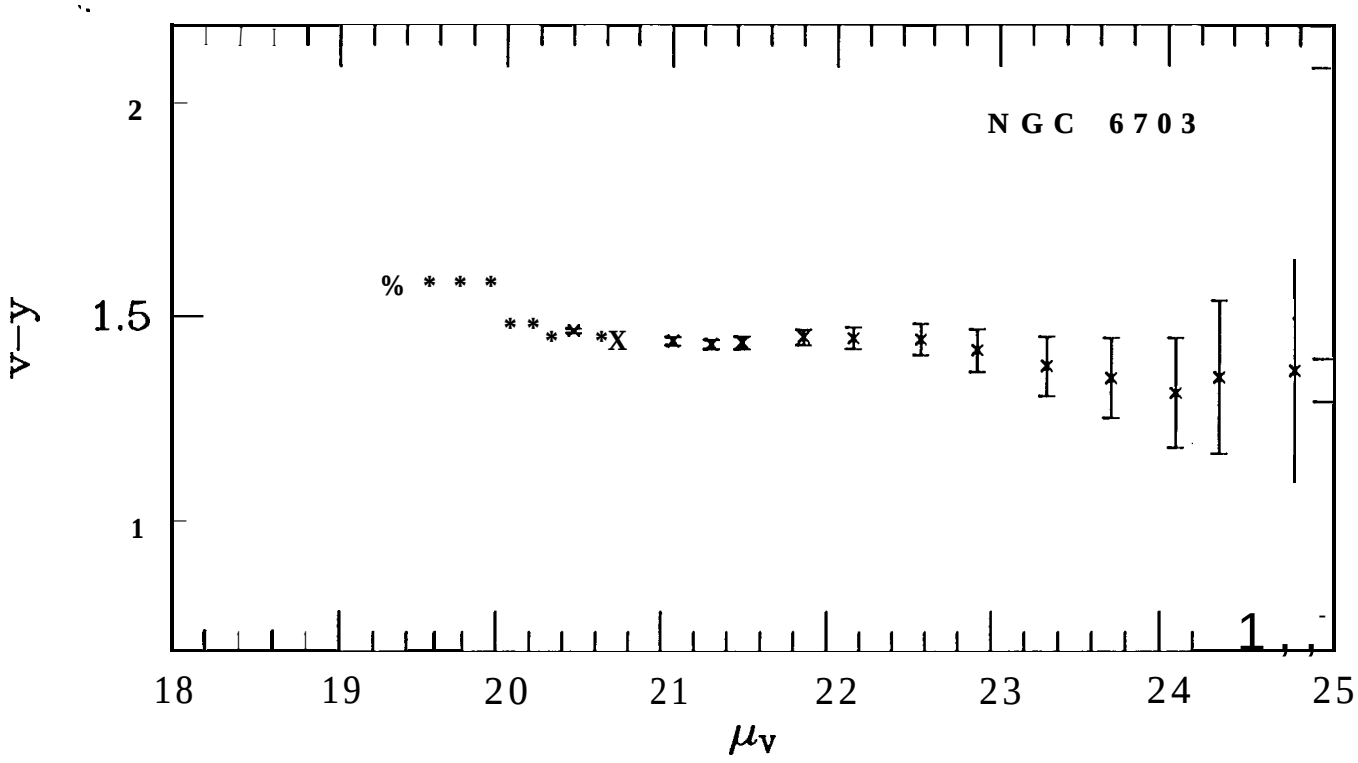
NGC 6703
v–y
2
1.5
1
18
19
20
21
22
23
24
25
μ_V

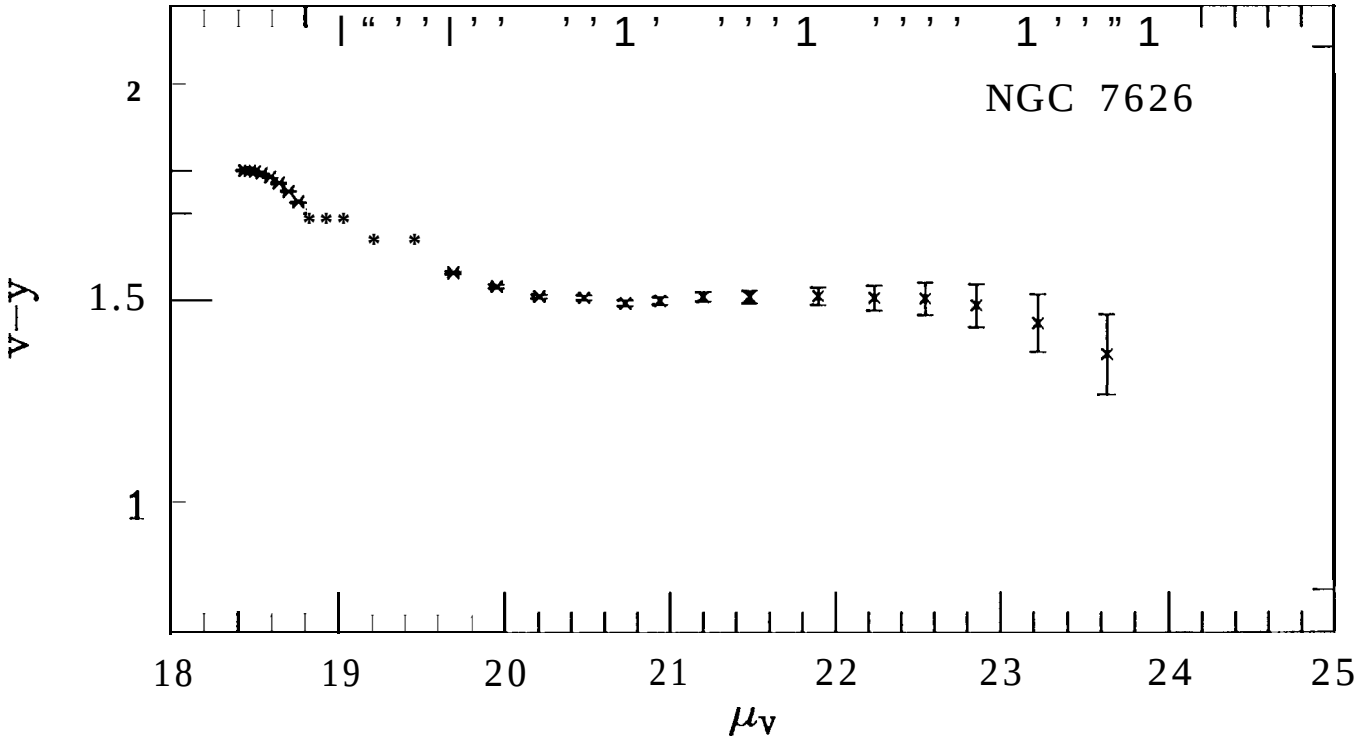
NGC 7626
v–y
2
1.5
1
18
19
20
21
22
23
24
25
μ_V

Figure 9

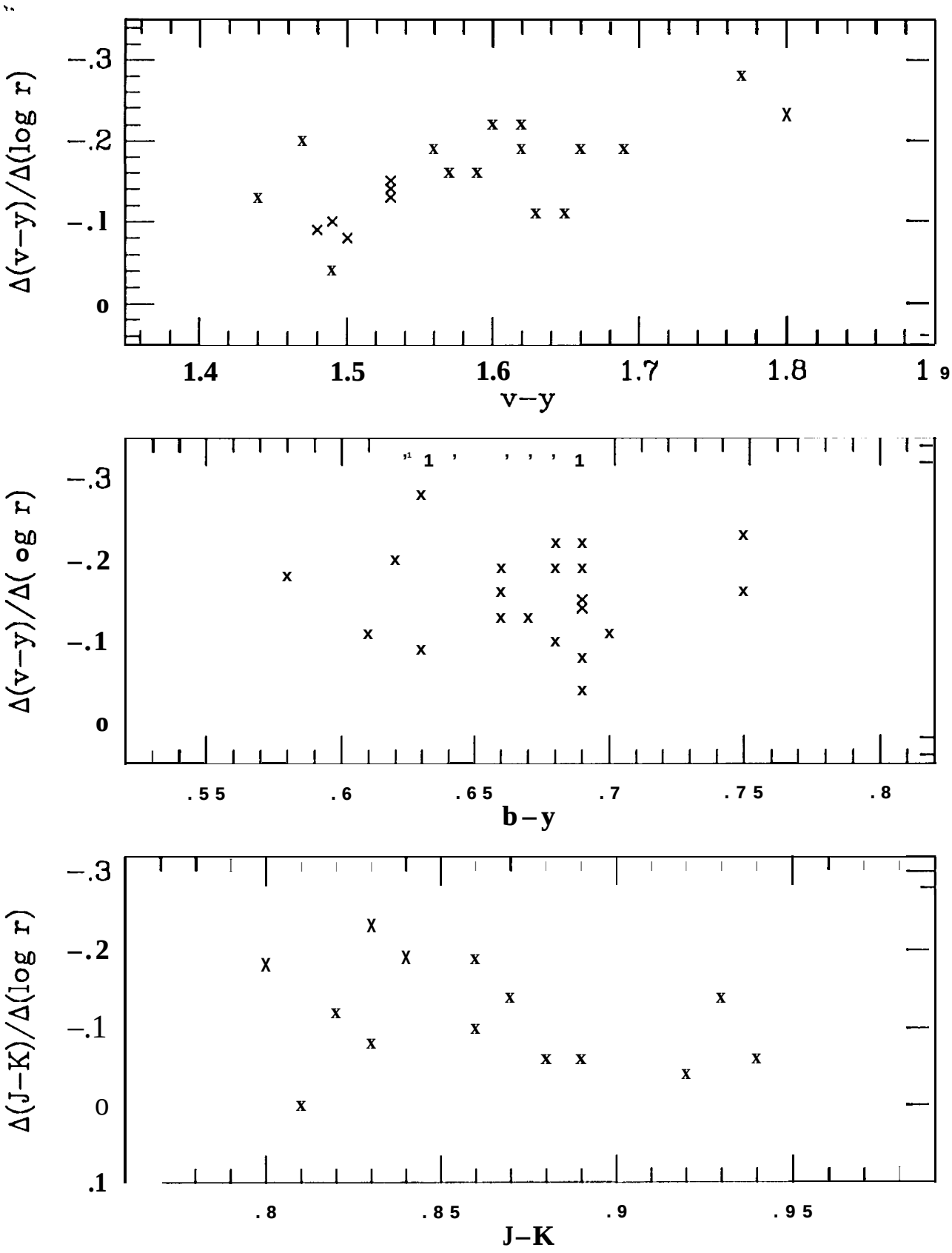
Δ(v−y)/Δ(log r)
−.3
−.2
−.1
0
1.4
1.5
1.6
1.7
1.8
v−y
Δ(v−y)/Δ(log r)
−.3
−.2
−.1
0
.55
.6
.65
.7
.75
.8
b−y
Δ(J−K)/Δ(log r)
−.3
−.2
−.1
0
.1
.8
.85
.9
.95
J−K

Figure 10

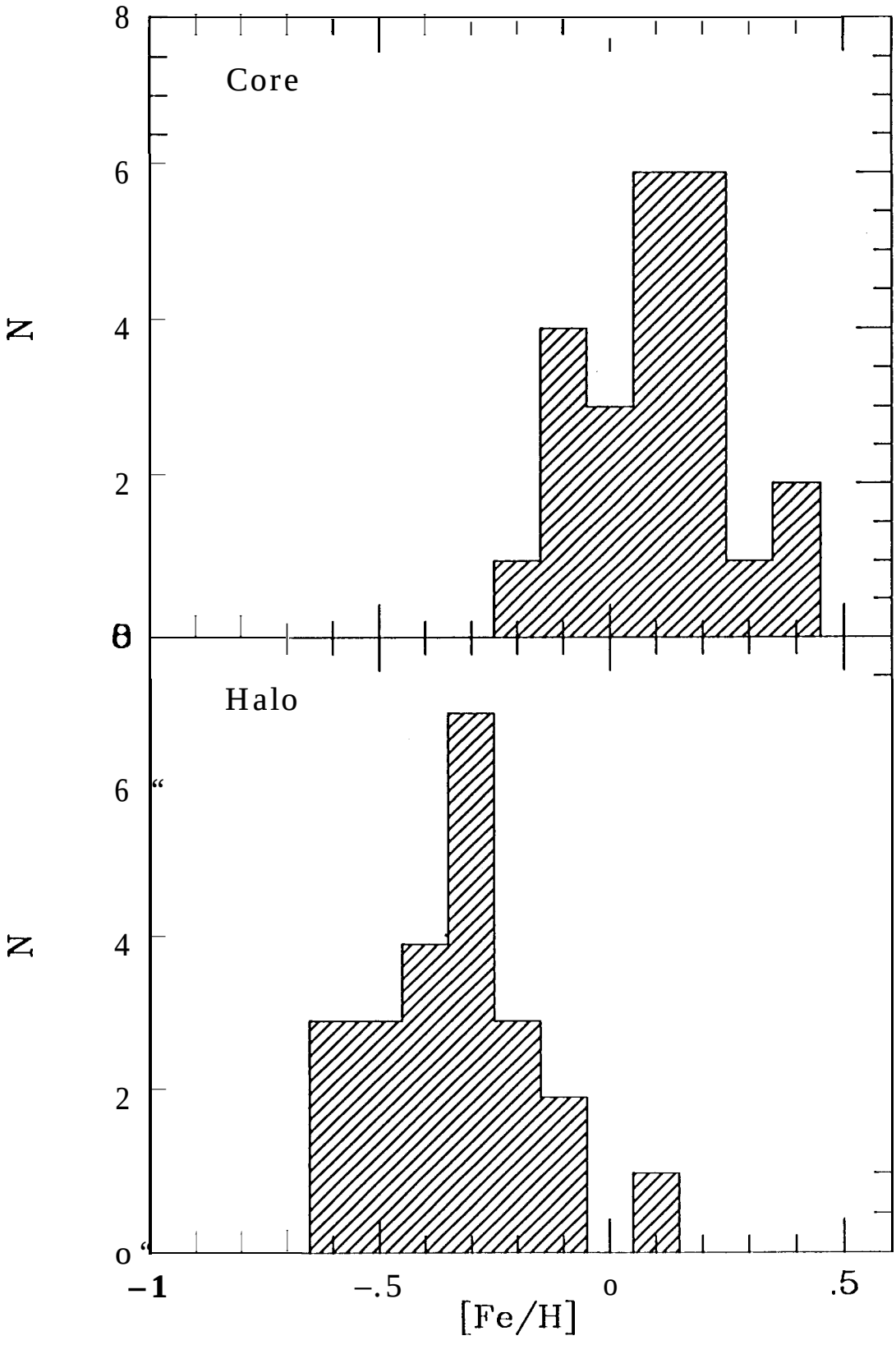

Figure 11